

SHEP 97/20

Heavy Quark Physics From Lattice QCD

J.M. Flynn and C.T. Sachrajda

Department of Physics and Astronomy, University of Southampton
Southampton SO17 1BJ, UK

Abstract

We review the application of lattice QCD to the phenomenology of b - and c -quarks. After a short discussion of the lattice techniques used to evaluate hadronic matrix elements and the corresponding systematic uncertainties, we summarise results for leptonic decay constants, B - \bar{B} mixing, semileptonic and rare radiative decays. A discussion of the determination of heavy quark effective theory parameters is followed by an explanation of the difficulty in applying lattice methods to exclusive nonleptonic decays.

To appear in Heavy Flavours (2nd edition)
edited by A.J. Buras and M. Lindner
(World Scientific, Singapore)

October 1997

HEAVY QUARK PHYSICS FROM LATTICE QCD

J.M. Flynn and C.T. Sachrajda

*Department of Physics and Astronomy, University of Southampton
Southampton SO17 1BJ, UK*

We review the application of lattice QCD to the phenomenology of b - and c -quarks. After a short discussion of the lattice techniques used to evaluate hadronic matrix elements and the corresponding systematic uncertainties, we summarise results for leptonic decay constants, B - \bar{B} mixing, semileptonic and rare radiative decays. A discussion of the determination of heavy quark effective theory parameters is followed by an explanation of the difficulty in applying lattice methods to exclusive nonleptonic decays.

1 Introduction

The lattice formulation of Quantum Chromodynamics (QCD) and large scale numerical simulations on parallel supercomputers are enabling theorists to evaluate the long-distance strong interaction effects in weak decays of hadrons in general, and of those containing a heavy (c - or b -) quark in particular. The difficulty in quantifying these non-perturbative QCD effects is the principal systematic error in the determination of the elements of the Cabibbo-Kobayashi-Maskawa (CKM) matrix from experimental measurements, and in using the data for tests of the standard model of particle physics and in searches for “new physics”. In this article we will review the main results obtained from lattice simulations in recent years, and discuss the principal sources of uncertainty and prospects for future improvements. More details can be found, for example, in the review talks presented at the annual symposia on lattice field theory (see Refs. ^{1–11}) and in references therein.

In the lattice formulation of quantum field theory space-time is approximated by a discrete “lattice” of points and the physical quantities of interest are evaluated numerically by computing the corresponding functional integrals. For these computations to make sense it is necessary for the lattice to be sufficiently large to accommodate the particle(s) being studied ($L \gg 1$ fm say, where L is the spatial length of the lattice), and for the spacing between neighbouring points (a) to be sufficiently small so that perturbation theory can be used to interpolate between the lattice points ($a\Lambda_{\text{QCD}} \ll 1$). The number of lattice points in a simulation is limited by the available computing resources; current simulations are performed with about 16–20 points in each spatial direction (up to about 64 points if the effects of quark loops are neglected, i.e. in the so called “quenched” approximation). Thus it is possible to work on

lattices which have a spatial extent of about 2 fm and a lattice spacing of 0.1 fm, perhaps satisfying the above requirements.

Since the Compton wavelength of heavy quarks is small, one has to be careful in their simulation. With a discretization of the Dirac action, $\bar{Q}(x)(\not{D} + m_Q)Q(x)$, where Q represents the field of the quark and m_Q its mass, the condition $a\Lambda_{\text{QCD}} \ll 1$ is not sufficient, one also requires $am_Q \ll 1$. Currently available lattices, in simulations performed in the quenched approximation, have spacings in the range $1.5 \text{ GeV} < a^{-1} < 4 \text{ GeV}$, and so it is not possible to simulate b -quarks directly in this way. Hence, one approach to B -physics is to simulate hadrons with heavy quarks which are still considered to be acceptably light (typically with masses in the range of that of the charmed quark), and then to extrapolate the results to the b -region, using scaling laws from the Heavy Quark Effective Theory (HQET) where applicable.

An important alternative approach is to use the HQET, and to compute physical quantities in terms of an expansion in inverse powers of the mass of the b -quark (and c -quark where appropriate). The first term in this expansion corresponds to a calculation using static (infinitely) heavy quarks. The evaluation of the coefficients in this expansion does not require propagating heavy quarks, and hence there are no errors of $O(m_Q a)$. However, as will be discussed in more detail in Section 5, the evaluation of the higher order terms in this expansion requires the subtraction of power divergences (i.e. terms which diverge as inverse powers of the lattice spacing a), which significantly reduces the precision which can be obtained.

In this article we focus on the decays of b - and c -quarks. Another important area of investigation is the spectroscopy of heavy quarkonia (for a review of recent results and references to the original literature see Ref. ¹²), in which the non-relativistic formulation of lattice QCD ¹³ is generally used.

The plan of this article is as follows. In the remainder of this Section we briefly review the general procedure used for evaluating hadronic matrix elements in lattice simulations and discuss the principal sources of uncertainty. The following Sections contain the status of the results for the leptonic decay constants f_B and f_D (Section 2), the B_B -parameter of B^0 - \bar{B}^0 mixing (Section 3), semileptonic decay amplitudes of B - and D -mesons (Section 4) and the parameters $\bar{\Lambda}$ (the binding energy of the heavy quark in a hadron), λ_1 (its kinetic energy) and λ_2 (the matrix element of the chromomagnetic operator) of the HQET (Section 5). Section 5 also contains a general discussion of the theoretical difficulties present in calculations of power corrections, i.e. corrections of $O(1/m_Q)$, $O(1/m_Q^2)$ etc., in physical quantities. Section 6 contains a brief summary of the status of lattice calculations of exclusive non-leptonic decay amplitudes, which is an area of investigation requiring considerable theoretical

Table 1: Where in this review to find results for some important physical quantities.

| Quantity | See. . . |
|--|--------------------------------------|
| Leptonic decay constants: $f_D, f_{D_s}, f_B, f_{B_s}$ | Eqs. (15–20) |
| Renormalization-group-invariant B -parameter for B - \bar{B} mixing, \hat{B}_B | Eq. (29) |
| $\xi \equiv f_{B_s} \hat{B}_{B_s}^{1/2} / f_{B_d} \hat{B}_{B_d}^{1/2}$ | Eq. (32) |
| Form factors $f^+(0), V(0), A_1(0)$ and $A_2(0)$ for semileptonic $D \rightarrow K, K^*, \pi, \rho$ decays | Table 8 |
| Form factor $f^+(0)$ and decay rate for $\bar{B}^0 \rightarrow \pi^+ l^- \bar{\nu}_l$ | Table 11 (UKQCD values) |
| Form factors $V(0), A_1(0)$ and $A_2(0)$ and rate for $\bar{B}^0 \rightarrow \rho^+ l^- \bar{\nu}_l$ | Table 12 (UKQCD values) |
| Form factor $T(0) \equiv T_1(0) = iT_2(0)$ for $\bar{B} \rightarrow K^* \gamma$ | Table 13 (UKQCD values) and Eq. (62) |

development. Finally in Section 7 we present a brief summary and outlook. Table 1 shows where our preferred estimates for some of the more important physical quantities can be found.

1.1 Evaluation of Hadronic Matrix Elements

By using the Operator Product Expansion, it is generally possible to separate the short- and long-distance contributions to weak decay amplitudes into Wilson coefficient functions and operator matrix elements respectively. Thus in order to evaluate the non-perturbative QCD effects it is necessary to compute the matrix elements of local composite operators. This is achieved in lattice simulations, by the direct computation of correlation functions of multi-local operators composed of quark and gluon fields (in Euclidean space):

$$\langle 0 | O(x_1, x_2, \dots, x_n) | 0 \rangle = \frac{1}{Z} \int [DA_\mu][D\psi][D\bar{\psi}] e^{-S} O(x_1, x_2, \dots, x_n) , \quad (1)$$

where Z is the partition function

$$Z = \int [DA_\mu][D\psi][D\bar{\psi}] e^{-S} , \quad (2)$$

S is the action and the integrals are over quark and gluon fields at each space-time point. In Eq. (1) $O(x_1, x_2, \dots, x_n)$ is a multi-local operator; the choice of O governs the physics which can be studied.

We now consider the two most frequently encountered cases, for which $n=2$ or 3. Let $O(x_1, x_2)$ be the bilocal operator

$$O_2(x_1, x_2) = T\{J_h(x_1)J_h^\dagger(x_2)\} , \quad (3)$$

where J_h is an interpolating operator for the hadron h whose properties we wish to study. In lattice computations we evaluate the two point correlation function

$$C_2(t_x) \equiv \sum_{\mathbf{x}} \langle 0 | O_2(x, 0) | 0 \rangle . \quad (4)$$

For sufficiently large positive t_x one obtains:

$$C_2(t_x) \simeq \frac{e^{-m_h t_x}}{2m_h} |\langle 0 | J_h(0) | h \rangle|^2 . \quad (5)$$

In Eq. (4) m_h is the mass of the hadron h , which is assumed to be the lightest one which can be created by the operator J_h^\dagger . The contribution from each heavier hadron, h' with mass $m_{h'}$ say, is suppressed by an exponential factor, $\exp(- (m_{h'} - m_h)t_x)$. In lattice simulations the correlation function C_2 is computed numerically, and by fitting the results to the expression in Eq. (5) both the mass m_h and the matrix element $\langle 0 | J_h(0) | h \rangle$ can be determined. In this case the hadron h is at rest, but of course it is also possible to give it a non-zero momentum, \mathbf{p} say, by taking the Fourier transform in Eq. (4) with the appropriate weighting factor $\exp(i\mathbf{p}\cdot\mathbf{x})$.

As an example consider the case in which h is the B -meson and J_h is the axial current A_μ (with the flavour quantum numbers of the B -meson). In this case one obtains the value of the leptonic decay constant f_B ,

$$\langle 0 | A_\mu(0) | B(p) \rangle = f_B p_\mu . \quad (6)$$

It will also be useful to consider three-point correlation functions:

$$C_3(t_x, t_y) = \sum_{\mathbf{x}, \mathbf{y}} e^{i\mathbf{p}\cdot\mathbf{x}} e^{i\mathbf{q}\cdot\mathbf{y}} \langle 0 | J_2(\mathbf{x}, t_x) O(\mathbf{y}, t_y) J_1^\dagger(\mathbf{0}, 0) | 0 \rangle , \quad (7)$$

where, J_1 and J_2 are the interpolating operators for hadrons h_1 and h_2 respectively, O is a local operator, and we have assumed that $t_x > t_y > 0$. Inserting complete sets of states between the operators in Eq. (7) we obtain

$$C_3(t_x, t_y) = \frac{e^{-E_1 t_y}}{2E_1} \frac{e^{-E_2(t_x - t_y)}}{2E_2} \langle 0 | J_2(\mathbf{0}, 0) | h_2(\mathbf{p}, E_2) \rangle \times \\ \langle h_2(\mathbf{p}, E_2) | O(\mathbf{0}, 0) | h_1(\mathbf{p} + \mathbf{q}, E_1) \rangle \langle h_1(\mathbf{p} + \mathbf{q}, E_1) | J_1^\dagger(\mathbf{0}, 0) | 0 \rangle + \dots, \quad (8)$$

where $E_1 = \sqrt{m_1^2 + (\mathbf{p} + \mathbf{q})^2}$, $E_2 = \sqrt{m_2^2 + \mathbf{p}^2}$ and the ellipsis represents the contributions from heavier states. The exponential factors, $\exp(-E_1 t_y)$ and $\exp(-E_2(t_x - t_y))$, assure that for large time separations, t_y and $t_x - t_y$, the contributions from the lightest states dominate. All the elements on the right-hand side of Eq. (8) can be determined from two-point correlation functions, with the exception of the matrix element $\langle h_2 | O | h_1 \rangle$. Thus by computing two- and three-point correlation functions the matrix element $\langle h_2 | O | h_1 \rangle$ can be determined.

The computation of three-point correlation functions is useful in studying semileptonic and radiative weak decays of hadrons, e.g. if h_1 is a B -meson, h_2 a D meson and O the vector current $\bar{b}\gamma^\mu c$, then from this correlation function we obtain the form factors relevant for semileptonic $B \rightarrow D$ decays.

We end this brief summary of lattice computations of hadronic matrix elements with a word about the determination of the lattice spacing a . It is conventional to introduce the parameter $\beta = 6/g_0^2(a)$, where $g_0(a)$ is the bare coupling constant in the theory with the lattice regularization. It is β (or equivalently $g_0(a)$) which is the input parameter in the simulation, and the corresponding lattice spacing is then determined by requiring that some physical quantity (which is computed in lattice units) is equal to the experimental value. For example, one may compute $m_\rho a$, where m_ρ is the mass of the ρ -meson, and determine the lattice spacing a by dividing the result by 769 MeV.

1.2 Sources of Uncertainty in Lattice Computations

Although lattice computations provide the opportunity, in principle, to evaluate the non-perturbative QCD effects in weak decays of heavy quarks from first principles and with no model assumptions or free parameters, in practice the precision of the results is limited by the available computing resources. In this section we outline the main sources of uncertainty in these computations:

- *Statistical Errors:* The functional integrals in Eq. (1) are evaluated by Monte-Carlo techniques. This leads to sampling errors, which decrease as

the number of field configurations included in the estimate of the integrals is increased.

- *Discretization Errors:* These are artefacts due to the finiteness of the lattice spacing. Much effort is being devoted to reducing these errors either by performing simulations at several values of the lattice spacing and extrapolating the results to the continuum limit ($a = 0$), or by “improving” the lattice formulation of QCD so that the error in a simulation at a fixed value of a is formally smaller^{14–17}. In particular, it has recently been shown to be possible to formulate lattice QCD in such a way that the discretization errors vanish quadratically with the lattice spacing¹⁸, even for non-zero quark masses¹⁹. This is in contrast with the traditional Wilson formulation²⁰, in which the errors vanish only linearly. Some of the simulations discussed in the following sections have used a tree-level improved action and operators; in these studies the artefacts formally vanish more quickly (like $a\alpha_s(a)$) than for the Wilson action. In the following, this tree-level improved action will be denoted as the SW (after Sheikholeslami-Wohlert who first proposed it¹⁶) or “clover” action.
- *Extrapolations to Physical Quark Masses:* It is generally not possible to use physical quark masses in simulations. For the light (u - and d -) quarks the masses must be chosen such that the corresponding π -mesons are sufficiently heavy to be insensitive to the finite volume of the lattice. In addition, as the masses of the quarks are reduced the computer time necessary to maintain the required level of precision increases rapidly. For the heavy quarks Q (i.e. for c , and particularly for b) the masses must be sufficiently small so that the discretization errors, which are of $O(m_Q a)$ or $O(m_Q^2 a^2)$, are small. The results obtained in the simulations must then be extrapolated to those corresponding to physical quark masses.
- *Finite Volume Effects:* We require that the results we obtain be independent of the size of the lattice. Thus, in principle, the spatial size of the lattice L should be $\gg 1$ fm (in practice $L \gtrsim 2$ -3 fm), and as mentioned above, we cannot use very light u - and d -quarks (in order to avoid very light pions whose correlation lengths, i.e. the inverses of their masses, would be of $O(L)$ or greater).
- *Contamination from Excited States:* These are the uncertainties due to the effects of the excited states, represented by the ellipsis in Eq. (5). In most simulations, this is not a serious source of error (it is, however, more significant in computations with static quarks). Indeed, by evaluating correlation functions $\langle J_h(x) J_h'(0) \rangle$ for a variety of interpolating operators

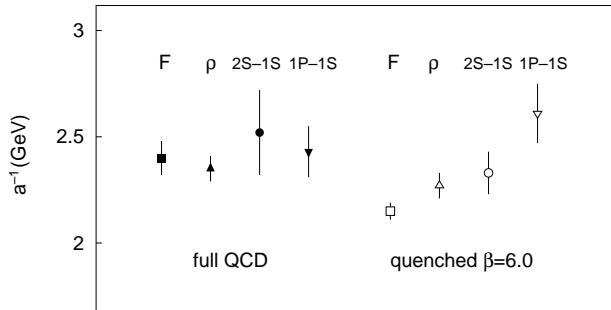


Figure 1: Comparison of lattice spacings (the quantity plotted is actually the *inverse* lattice spacing, a^{-1}) determined from different physical quantities in quenched and unquenched simulations by the SESAM and T χ L collaborations²⁵. F denotes the value determined from the static quark potential and ρ denotes the value determined from the ρ -meson mass, while 2S-1S and 1P-1S denote values obtained from energy level splittings in $Q\bar{Q}$ bound states using the lattice formulation of nonrelativistic QCD.

$\{J_h, J'_h\}$, it is possible to obtain the masses and matrix elements of the excited hadrons (for a recent example see²¹).

- *Lattice-Continuum Matching*: The operators used in lattice simulations are bare operators defined with the lattice spacing as the ultra-violet cut-off. From the matrix elements of the bare lattice composite operators, we need to obtain those of the corresponding renormalized operators defined in some standard continuum renormalization scheme, such as the $\overline{\text{MS}}$ scheme. The relation between the matrix elements of lattice and continuum composite operators involves only short-distance physics, and hence can be obtained in perturbation theory. Experience has taught us, however, that the coefficients in lattice perturbation theory can be large, leading to significant uncertainties (frequently of $O(10\%)$ or more). For this reason, non-perturbative techniques to evaluate the renormalization constants which relate the bare lattice operators to the renormalized ones have been developed, using chiral Ward identities where possible²² or by imposing an explicit renormalization condition²³ (see also Refs.^{18,24}), thus effectively removing this source of uncertainty in many important cases.
- *“Quenching”*: In most current simulations the matrix elements are evaluated in the “quenched” approximation, in which the effects of virtual quark loops are neglected. For each gluon configuration $\{U_\mu(x)\}$, the functional integral over the quark fields in Eq. (1) can be performed formally, giving the determinant of the Dirac operator in the gluon background field

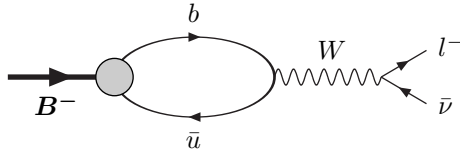


Figure 2: Diagram representing the leptonic decay of the B -meson.

corresponding to this configuration. The numerical evaluation of this determinant is possible, but is computationally very expensive, and for this reason the determinant is frequently set equal to its average value, which is equivalent to neglecting virtual quark loops. Gradually, however, unquenched calculations are beginning to be performed, e.g. in Figure 1 we show the lattice spacing obtained by the SESAM and T χ L collaborations from four physical quantities in both quenched and unquenched simulations²⁵. In the quenched case there is a spread of results of about $\pm 10\%$, whereas in the unquenched case the spread is smaller (although the errors are still sizeable for some of the quantities used). In the next 3–5 years it should be possible to compute most of the physical quantities discussed below without imposing this approximation.

2 The Leptonic Decay Constants f_D and f_B

In this section we review the current status of calculations of the leptonic decay constants f_D and f_B . Leptonic decays of heavy mesons, see Figure 2, are particularly simple to treat theoretically^a. In each case the strong interaction effects are contained in a single parameter, called the decay constant, f_D or f_B . Parity symmetry implies that only the axial component of the V – A weak current contributes to the decay, and Lorentz invariance that the matrix element of the axial current is proportional to the momentum of the meson (with the constant of proportionality defined to be the decay constant) as, for example, in Eq. (6).

Knowledge of f_B would allow us to predict the rates for the corresponding decays:

$$\Gamma(B \rightarrow l\nu_l + l\nu_l\gamma) = \frac{G_F^2 V_{ub}^2}{8\pi} f_B^2 m_l^2 m_B \left(1 - \frac{m_l^2}{m_B^2}\right)^2 (1 + O(\alpha)), \quad (9)$$

where the $O(\alpha)$ corrections are also known. The value of f_B is very important

^aFor simplicity, the presentation here is for pseudoscalar mesons D and B . A parallel discussion holds also for the vector mesons D^* and B^* .

Table 2: Results for f_D and f_{D_s} using the conventional formulation of heavy quarks. All values were obtained in the quenched approximation, except for those from the HEMCGC collaboration which were computed for two flavours of sea quarks ($n_f = 2$) (we have combined quoted systematic errors from HEMCGC in quadrature). Infinite values of β symbolise results obtained after extrapolation to the continuum limit. The error quoted by APE includes an estimate of discretization uncertainties taken from a comparison of results at $\beta = 6.0$ and 6.2. Results from MILC and JLQCD are preliminary.

| | Yr | β | c_{sw} | norm | f_D/MeV | f_{D_s}/MeV | f_{D_s}/f_D |
|----------------------|----|----------|-----------------|------|---|---|---|
| MILC ²⁶ | 97 | ∞ | 0 | nr | 186(10) ⁽²⁷⁾ ₍₁₈₎ ⁽⁹⁾ ₍₀₎ | 199(8) ⁽⁴⁰⁾ ₍₁₁₎ ⁽¹⁰⁾ ₍₀₎ | 1.09(2) ⁽⁵⁾ ₍₁₎ ⁽²⁾ ₍₀₎ |
| JLQCD ²⁷ | 97 | ∞ | 0,1 | nr | 192(10) ⁽¹¹⁾ ₍₁₆₎ | 213(11) ⁽¹²⁾ ₍₁₈₎ | |
| APE ²⁸ | 97 | 6.2 | 1 | rel | 221(17) | 237(16) | 1.07(4) |
| LANL ²⁹ | 96 | 6.0 | 0 | nr | 229(7) ⁽²⁰⁾ ₍₁₆₎ | 260(4) ⁽²⁷⁾ ₍₂₂₎ | 1.135(2) ⁽⁶⁾ ₍₂₃₎ |
| LANL ²⁹ | 96 | ∞ | 0 | nr | 186(29) | 218(15) | |
| PCW ³⁰ | 94 | ∞ | 0 | nr | 170(30) | | 1.09(2)(5) |
| UKQCD ³¹ | 94 | 6.2 | 1 | rel | 185 ⁽⁴⁾ ₍₃₎ ⁽⁴²⁾ ₍₇₎ | 212 ⁽⁴⁾ ₍₄₎ ⁽⁴⁶⁾ ₍₇₎ | 1.18(2) |
| UKQCD ³¹ | 94 | 6.0 | 1 | rel | 199 ⁽¹⁴⁾ ₍₁₅₎ ⁽²⁷⁾ ₍₁₉₎ | 225 ⁽¹⁵⁾ ₍₁₅₎ ⁽³⁰⁾ ₍₂₂₎ | 1.13 ⁽⁶⁾ ₍₇₎ |
| BLS ³² | 94 | 6.3 | 0 | nr | 208(9)(35)(12) | 230(7)(30)(18) | 1.11(6) |
| HEMCGC ³³ | 94 | 5.3 | 0 | nr | 215(5)(53) | 287(5)(60) | |
| HEMCGC ³⁴ | 93 | 5.6 | 0 | | 200–287 | 220–320 | |
| ELC ³⁵ | 92 | 6.4 | 0 | rel | 210(40) | 230(50) | |
| PCW ³⁶ | 91 | 6.0 | 0 | rel | 198(17) | 209(18) | |
| ELC ³⁷ | 88 | 6.2 | 0 | rel | 181(27) | 218(27) | |
| ELC ³⁷ | 88 | 6.0 | 0 | rel | 197(14) | 214(19) | |
| DeGL ³⁸ | 88 | 6.0 | 0 | rel | 190(33) | 222(16) | 1.17(22) |
| BDHS ³⁹ | 88 | 6.1 | 0 | rel | 174(26)(46) | 234(46)(55) | 1.35(22) |

in describing $B-\bar{B}$ mixing as explained in Section 3. Knowing f_B would also be useful for our understanding of other processes in B -physics, particularly those for which “factorization” turns out to be a useful approximation.

Lattice results for decay constants of charmed and bottom mesons obtained over the last ten years are summarised in Tables 2 and 3. These are presented using a normalization in which $f_{\pi^+} \simeq 131$ MeV.

Since we are dealing with a heavy quark with mass m_Q , the product $m_Q a$ is large and can be an important source of mass-dependent discretization errors. This has been addressed in two ways in the decay constant calculations from 1994 onwards. Some studies, denoted by $c_{\text{sw}} = 1$, have used the Sheikholeslami-Wohlert (SW or clover) improved action¹⁶ together with improved operators¹⁷, which removes tree level $O(a)$ errors, leaving ones of $O(\alpha_s m_Q a)$. In the near future we can look forward to the application of re-

Table 3: Results for f_B and f_{B_s} using the conventional formulation of heavy quarks. All values were obtained in the quenched approximation, except for those from the HEMCGC collaboration which were computed with two flavours of sea quarks ($n_f = 2$) (we have combined quoted systematic errors from HEMCGC in quadrature). Infinite values of β symbolise results obtained after extrapolation to the continuum limit. The error quoted by APE includes an estimate of discretization uncertainties taken from a comparison of results at $\beta = 6.0$ and 6.2 . Results from MILC and JLQCD are preliminary.

| | Yr | β | c_{sw} | norm | f_B/MeV | f_{B_s}/MeV | f_{B_s}/f_B |
|----------------------|----|----------|----------|------|--------------------------------------|-------------------------------------|-------------------------------------|
| MILC ²⁶ | 97 | ∞ | 0 | nr | 153(10)($^{36}_{13}$)($^{13}_0$) | 164(9)($^{47}_{13}$)($^{16}_0$) | 1.10(2)($^{5}_{3}$)($^{3}_{2}$) |
| JLQCD ²⁷ | 97 | ∞ | 0,1 | nr | 163(12)($^{13}_{16}$) | 180(16)($^{14}_{18}$) | |
| APE ²⁸ | 97 | 6.2 | 1 | rel | 180(32) | 205(35) | 1.14(8) |
| PCW ³⁰ | 94 | ∞ | 0 | nr | 180(50) | | 1.09(2)(5) |
| UKQCD ³¹ | 94 | 6.2 | 1 | rel | 160(6)($^{59}_{19}$) | 194($^{6}_{5}$)($^{62}_{9}$) | 1.22($^{4}_{3}$) |
| UKQCD ³¹ | 94 | 6.0 | 1 | rel | 176($^{25}_{24}$)($^{33}_{15}$) | | 1.17(12) |
| BLS ³² | 94 | 6.3 | 0 | nr | 187(10)(34)(15) | 207(9)(34)(22) | 1.11(6) |
| HEMCGC ³³ | 94 | 5.3 | 0 | nr | 150(10)(57) | | |
| HEMCGC ³⁴ | 93 | 5.6 | 0 | | 152–235 | | |
| ELC ³⁵ | 92 | 6.4 | 0 | rel | 205(40) | | |
| BDHS ³⁹ | 88 | 6.1 | 0 | rel | 105(17)(30) | | |

cently developed techniques to reduce the discretization errors still further, to ones of $O(m_Q^2 a^2)$ ^{18,19}. The second approach introduces a revised normalization of the quark fields in simulations using the standard Wilson fermion action. This is designed to remove higher order effects in $m_Q a$ from the heavy quark propagator, but only at tree level in the strong interactions, and is distinguished in the table by the label ‘nr’, denoting a nonrelativistic normalization (in contrast to the standard ‘rel’ or relativistic one). The theoretical significance of this normalization factor is not completely clear; in particular, it does not eliminate all the $O(m_Q a)$ effects. The nonrelativistic normalization is often denoted ‘KLM’ in the literature, after some of its originators^{2,40–43}. For more details of the lattice formulations and improvement procedures, see the recent review by Wittig⁴⁴.

The main efforts of the lattice community are being devoted to controlling the systematic uncertainties, which dominate the errors. This is illustrated by the latest, and still preliminary, results, which come from the MILC²⁶ and JLQCD²⁷ collaborations. These collaborations are carrying out extensive simulations using many different lattice spacings to allow them to extrapolate to the continuum limit. JLQCD study different prescriptions for reducing the $O(m_Q a)$ discretization errors associated with heavy quarks with the aim of

demonstrating that all results converge in the continuum limit. Their error is statistical combined with the uncertainty due to the spread over prescriptions. In Figure 3 we show the continuum extrapolation of their results for f_D and f_B for two different lattice fermion formulations. In this case the continuum values of f_B and f_D obtained using the two formulations agree remarkably well; the agreement is still acceptable (although not so remarkable) when quantities other than the string tension are used to determine the lattice spacing. We also note that in this case the dependence on the lattice spacing is milder for the improved action as expected (although further studies are needed to confirm whether this is a general feature).

MILC simulate a range of heavy quark masses, giving meson masses straddling m_D , together with a static (infinite mass) quark, allowing an interpolation to m_B . The continuum extrapolation of their results is illustrated in Figure 4. In the MILC results, the first error is statistical and the second is systematic within the quenched approximation. MILC also have some unquenched simulation results (with $n_f = 2$ dynamical flavours). Their final error is for the effects of quenching, which they estimate from: (i) the difference between the unquenched results at the smallest available lattice spacing and the quenched results interpolated to the same spacing, and (ii) comparing the results when the lattice spacing is fixed by f_π or m_ρ .^b Their results suggest that unquenching may raise the value of the decay constants. This agrees with estimates^{45,46}, using the difference between chiral loop contributions in quenched and unquenched QCD, that f_B and f_{B_s} in full QCD are increased by 10–20% over their quenched values. Lattice simulations are possible using scalar fields with a quark-like action which act effectively as negative numbers of ordinary quark flavours⁴⁷. Calculations of f_B in the static limit extrapolated from negative numbers of flavours also suggest an increase of about 20%.

At this point we feel we need to add a word of caution. In their evaluation of f_B , both the JLQCD and MILC collaborations simulate heavy quarks with masses m_Q satisfying $m_Q a > 1$ and apply a nonrelativistic or ‘KLM’ normalization prescription. Even with such a normalization, however, one should worry about the discretization errors when such large masses are used. Not only would one expect these errors to be sizeable at a fixed value of beta, but the extrapolation to the continuum limit is now complicated since all powers of $m_Q a$ contribute significantly to the results which are being extrapolated. Set against these worries is the observation by the MILC collaboration that they obtain very similar values for f_B if they restrict the set of points to be extrapolated to those with heavy quarks with reasonably small masses (the differences

^bFor f_{D_s} and f_{B_s} they also compare results where the strange quark mass is determined by m_K or m_ϕ .

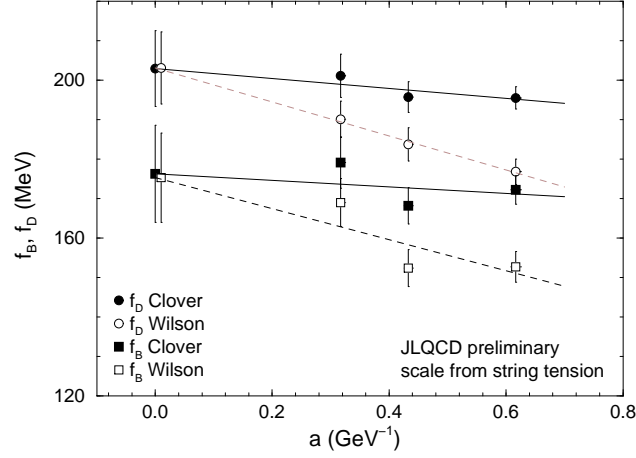


Figure 3: Continuum extrapolation of JLQCD²⁷ results (preliminary) for f_D and f_B . The graph shows agreement between results from two different lattice formulations when extrapolated to zero lattice spacing. Open symbols denote an unimproved Wilson action ($c_{sw} = 0$), filled symbols denote an improved Sheikholeslami-Wohlert or Clover ($c_{sw} = 1$) action.

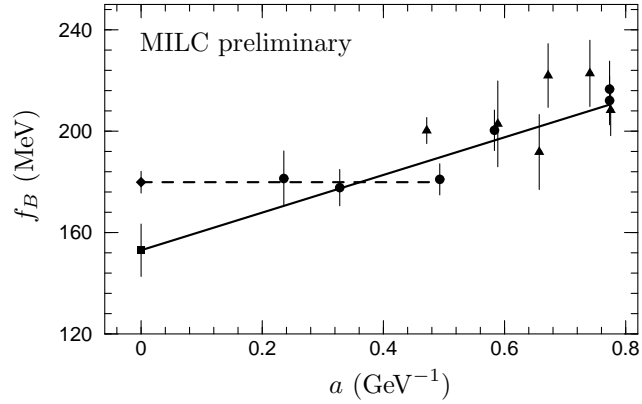


Figure 4: Continuum extrapolation of MILC²⁶ results (preliminary) for f_B . Circles (triangles) denote results from quenched (unquenched $n_f = 2$) simulations. The solid line and square denote the continuum extrapolation by a linear fit in the lattice spacing a to the quenched results, while the dashed line and diamond denote a weighted average of the three quenched results at smallest a . The scale is set by f_π .

are included in their error bars). Our own strong preference is to restrict the simulations to heavy quarks with masses significantly smaller than 1 in lattice units (and to use improved actions).

In obtaining a continuum value for f_B one has to decide in what order to perform the extrapolations in a and m_Q . The MILC collaboration obtain f_B by fitting, at each finite lattice spacing a , the value of the decay constant of a static quark (infinite mass) and those of several mesons with finite masses (it should be noted that these have different systematic errors). They then extrapolate the results for f_B to the continuum limit to obtain their final result. An alternative procedure^{30,44,48} is to perform separately the continuum extrapolations of the static results and results obtained at fixed finite meson masses. The mass dependence of the continuum points is then fitted to determine the physical decay constants. The most recent analysis using this method has been performed by Wittig⁴⁴, combining lattice data from many simulations. The MILC and JLQCD data is excluded, since it is still preliminary, and the results obtained with the clover action have also not been included since it was felt that there is insufficient data to perform the continuum extrapolation. This analysis shows some evidence for discretization errors at large quark masses, where results using different normalization procedures, mass definitions and so on, begin to diverge. Wittig's final fit, therefore, is to the static point and to points with meson masses less than about 2 GeV. The results of this procedure give⁴⁴

$$f_D = 191 \pm_{28}^{19} \text{ MeV} \quad (10)$$

$$f_{D_s} = 206 \pm_{28}^{18} \text{ MeV} \quad (11)$$

$$f_B = 172 \pm_{31}^{27} \text{ MeV} \quad (12)$$

The statistical error and the systematic error arising from fixing the lattice spacing are the dominant (and comparable) uncertainties in these numbers. The central values are obtained using the continuum extrapolated value of f_π to fix the lattice spacing⁴⁴.

The dimensionless ratios f_{D_s}/f_D and f_{B_s}/f_B are also of great interest and have the advantage that many systematic effects should partially cancel. The lattice results illustrate, as expected, that the value of the decay constant decreases as the mass of the light valence quark decreases. Here a straightforward extrapolation of world results by Wittig⁴⁴ gives

$$f_{D_s}/f_D = 1.08 \pm 0.08, \quad (13)$$

$$f_{B_s}/f_B = 1.14 \pm 0.08, \quad (14)$$

which are compatible with the preliminary MILC results²⁶. These results are obtained in the quenched approximation. MILC estimate the quenching error

in the ratios to be about 3%. One would expect a small correction here from cancellation of the effects in f_{B_s} and f_B separately. We note that the chiral loop estimate for the difference of the ratio f_{B_s}/f_B from 1 can be surprisingly large^{45,46}, e.g. for one choice of parameters it can be as large as +16%.

2.1 Summary and Conclusions

We now summarise this rather lengthy discussion and present our conclusions. The two principle sources of uncertainty in the calculations of the decay constants are those due to discretization errors and to quenching. The effects of the latter are only now beginning to be studied, and early indications suggest that the values of the decay constants may increase when the effects of quark loops are fully included, but this still needs to be confirmed. The discretization errors are currently studied either by using improved actions and operators, or by performing the computations at a sequence of lattice spacings and extrapolating the results to the continuum limit. The results from the two approaches are consistent, and further confirmation that these errors are under control will come after the implementation of the $O(a^2)$ improvement techniques proposed in Refs.^{18,19}. Our view of the current status of the calculations can be summarised by the following values for the decay constants and their ratios:

$$f_D = 200 \pm 30 \text{ MeV} \quad (15)$$

$$f_{D_s} = 220 \pm 30 \text{ MeV} \quad (16)$$

$$f_B = 170 \pm 35 \text{ MeV} \quad (17)$$

$$f_{B_s} = 195 \pm 35 \text{ MeV} \quad (18)$$

$$f_{D_s}/f_D = 1.10 \pm 0.06 \quad (19)$$

$$f_{B_s}/f_B = 1.14 \pm 0.08 \quad (20)$$

The principal difficulty in presenting results for physical quantities such as those in Eqs. (15–20) is to estimate the errors. The value of the lattice spacing typically varies by 10% or so depending on which physical quantity is used to calibrate the lattice simulation. This variation is largely due to the use of the quenched approximation. We therefore consider that $\pm 10\%$ is an irreducible minimum error in decay constants computed in quenched simulations (15% when they are computed in the static limit, since in that case it is $f_B\sqrt{m_B}$ which is computed directly). The remainder of each error in Eqs. (15–20) and below is based on our estimates of the other uncertainties, particularly those due to discretization errors and the normalization of the lattice composite operators. As explained in the Introduction, much successful work is currently being done to reduce these uncertainties.

It is very interesting to compare the lattice *prediction* for f_{D_s} in Eq. (16) with experimental measurements. Combining four measurements of f_{D_s} from $D_s \rightarrow \mu\nu$ decays, the rapporteur at the 1996 ICHEP conference found⁴⁹

$$f_{D_s} = 241 \pm 21 \pm 30 \text{ MeV}. \quad (21)$$

In spite of the sizeable errors, the agreement with the lattice prediction is very pleasing and gives us further confidence in the predictions for f_B and related quantities.

We end this section with a comment on the validity of the asymptotic scaling law for the decay constants. For sufficiently large masses of the heavy quark, the decay constant of a heavy-light pseudoscalar meson P scales with its mass m_P as follows:

$$f_P = \frac{A}{\sqrt{m_P}} \left[\alpha_s(m_P)^{-2/\beta_0} \{1 + O(\alpha_s(m_P))\} + O\left(\frac{1}{m_P}\right) \right], \quad (22)$$

where A is independent of m_P . Using the leading term of this scaling law, a value of 200 MeV for f_D would correspond to $f_B \simeq 120$ MeV. Results from the lattice computations shown in Table 3, however, indicate that f_B is significantly larger than this and that the $O(1/m_P)$ corrections on the right-hand side of Eq. (22) are considerable. The coefficient of the $O(1/m_P)$ corrections is typically found to be between 0.5 and 1 GeV, on the large side of theoretical expectations.

3 $B^0 - \bar{B}^0$ Mixing

$B-\bar{B}$ mixing provides important constraints for the determination of the angles of the unitarity triangle (for a review and references to the original literature see e.g. Ref.⁵⁰). In this process, the strong interaction effects are contained in the matrix element of the $\Delta B=2$ operator:

$$M(\mu) = \langle \bar{B}^0 | \bar{b}\gamma_\mu(1-\gamma_5)q \bar{b}\gamma^\mu(1-\gamma_5)q | B^0 \rangle, \quad (23)$$

where $q=d$ or s (unless indicated otherwise, we assume that $q=d$). The argument μ implies that the operator has been renormalized at the scale μ . It is conventional to introduce the B_B -parameter through the definition

$$M(\mu) = \frac{8}{3} f_B^2 m_B^2 B_B(\mu). \quad (24)$$

The dimensionless quantity B_B is better-determined than f_B in lattice calculations, so that the theoretical uncertainties in the value of the matrix element M , needed for phenomenology, are dominated by our ignorance of f_B .

Table 4: Results for the mixing parameter B_B obtained in the quenched approximation using static b -quarks (the value for c_{sw} refers to the light quark action). $B_B(m_b)$ with $m_b = 5 \text{ GeV}$ is calculated from the raw lattice matrix elements and then converted to \hat{B}_B^{nlo} , the renormalization group invariant B -parameter. For ease of comparison we have used the same choice of parameters in all cases together with NLO matching from lattice to continuum. Where this has changed the results from those quoted by the authors, the result obtained by us is indicated in oblique type. M1, M2 and M3 denote three different but equivalent ways of organising the matching calculations (see text).

| | Yr | β | c_{sw} | | $B_B(m_b)$ | \hat{B}_B^{nlo} |
|---------------------|----|---------|-----------------|----|------------|--------------------------|
| GM ⁵² | 97 | 6.0 | 1 | M1 | 0.76(5) | 1.21(8) |
| | | | | M2 | 0.54(4) | 0.86(6) |
| | | | | M3 | 0.86(5) | 1.37(8) |
| UKQCD ⁵⁴ | 96 | 6.2 | 1 | M1 | 0.76(6) | 1.20(9) |
| | | | | M2 | 0.57(6) | 0.91(9) |
| | | | | M3 | 0.82(6) | 1.31(9) |
| Ken ⁵³ | 96 | 6.0 | 0 | M1 | 0.93(4) | 1.48(7) |
| | | | | M2 | 0.75(4) | 1.19(7) |
| | | | | M3 | 0.98(4) | 1.56(7) |

$B_B(\mu)$ is a scale dependent quantity for which lattice results are most often quoted after translation to the $\overline{\text{MS}}$ scheme. The next-to-leading order (NLO) renormalization group invariant B -parameter (\hat{B}_B^{nlo}) is defined by

$$\hat{B}_B^{\text{nlo}} = \alpha_s(\mu)^{-2/\beta_0} \left(1 + \frac{\alpha_s(\mu)}{4\pi} J_{n_f} \right) B_B(\mu), \quad (25)$$

where $\beta_0 = 11 - 2n_f/3$ and J_{n_f} is obtained from the one- and two-loop anomalous dimensions of the $\Delta B=2$ operator by⁵¹,

$$J_{n_f} = \frac{1}{2\beta_0} \left(\gamma_0 \frac{\beta_1}{\beta_0} - \gamma_1 \right), \quad (26)$$

with $\beta_1 = 102 - 38n_f/3$, $\gamma_0 = 4$ and $\gamma_1 = -7 + 4n_f/9$. In the discussion below we choose $\mu = m_b$.

Results for B_B are summarised in Table 4 for static b quarks and in Table 5 for propagating b -quarks. We now discuss these two cases in turn.

3.1 B_B obtained using static b -quarks

The main difficulty in trying to determine the value of B_B using static heavy quarks is due to the large perturbative corrections which are encountered when

calculating the matrix element $M(\mu)$ in some standard renormalization scheme (e.g. the $\overline{\text{MS}}$ scheme) in full QCD from those measured on the lattice in the effective theory. We will illustrate this below. Because of the relatively large uncertainties which result from the truncation of the perturbation series, we believe that, at present, the calculations of B_B in the static theory add little to the information obtained with propagating quarks. For this reason our “best” lattice value for B_B is obtained using results obtained with propagating quarks only, and will be presented in section 3.2 below.

In order to compute $M(m_b)$ one needs to evaluate the matrix elements of four $\Delta B = 2$ operators in the static lattice theory (denoted by $O_i(a)$ with $i = L, N, R, S$). The relation between $M(m_b)$ and the matrix elements of the O_i is of the form:

$$M(m_b) = \sum_{i=L,N,R,S} Z_i(m_b, a) \langle O_i(a) \rangle. \quad (27)$$

The explicit form of the operators and details of the matching can be found in Refs. ^{55–59}. The matching can be performed in three stages:

- (i) From the matrix elements of the lattice operators in the effective theory one can obtain the corresponding ones renormalized in some standard continuum scheme at a scale $\mu = a^{-1}$.
- (ii) Using the renormalization group equations one then obtains the continuum effective theory matrix elements of operators renormalized at a scale $\mu = m_b$.
- (iii) Finally, by matching the continuum effective theory and full QCD one obtains $M(m_b)$.

We illustrate this procedure by considering Z_L , which in practice is the most complicated case (the operator O_L is just that in Eq. (23) but with static heavy quarks). It can be written in the form:

$$Z_L = \left\{ C_L(m_b) \left(\frac{\alpha_s(m_b)}{\alpha_s(a^{-1})} \right)^{d_1} \left(1 + \frac{\alpha_s(a^{-1}) - \alpha_s(m_b)}{4\pi} J \right) + C_S(m_b) \left[\left(\frac{\alpha_s(m_b)}{\alpha_s(a^{-1})} \right)^{d_2} - \left(\frac{\alpha_s(m_b)}{\alpha_s(a^{-1})} \right)^{d_1} \right] K \right\} \left(1 + \frac{\alpha_s(a^{-1})}{4\pi} D_L \right), \quad (28)$$

where J and K are constants obtained from the anomalous dimension matrix of the operators O_L and O_S in the continuum effective theory, and D_L is a constant (which arises in step (i) of the matching procedure). The terms

containing both the scales m_b and a^{-1} in Eq. (28) arise from the evolution in step (ii) and the coefficients C_L and C_S from the matching in step (iii).

To obtain B_B we divide the result for $M(m_b)$ by f_B^2 , and so in the denominator there is a factor of Z_A^2 , where Z_A is the constant relating the physical axial current to that in the lattice static theory. Z_A is also calculated in perturbation theory.

We consider three methods which have recently been used to treat the perturbative corrections; these methods differ only at higher orders in perturbation theory for which the coefficients are unknown. They are therefore equivalent at NLO. Because some of the coefficients in the Z_i 's are large, this leads to significant uncertainties in the result for B_B . The three methods are:

M1: the expressions for each of the Z_i are evaluated exactly as in the example of Eq. (28),

M2: the terms of $O(\alpha_s^2)$ in each Z_i are dropped ($i = L, N, R, S, A$),

M3: the terms of $O(\alpha_s^2)$ in each Z_i/Z_A^2 are dropped ($i = L, N, R, S$).

M1 and M2 are the methods used by Giménez and Martinelli in ⁵², while M3 is the “fully-linearised” method of the Kentucky group ⁵³.

For the numerical estimates in Table 4 we adopt the same choice of parameters as Giménez and Martinelli in ⁵², using $\Lambda_{\overline{\text{MS}}}^{(4)} = 200$ MeV, $n_f = 4$ and $m_b = 5$ GeV for the lattice-to-continuum matching to find $B_B(m_b)^c$. To obtain \hat{B}_B^{nlo} we set $n_f = 5$ in Eq. (25) and keep α_s continuous at the threshold at m_b . Where necessary, we have taken the raw matrix elements from the different groups and have simply propagated the errors in the linear combination which determines B_B .

As Table 4 shows, because of the large coefficients, there are significant differences between the formally equivalent procedures M1, M2 and M3. Furthermore, the results from UKQCD ⁵⁴ and Giménez and Martinelli ⁵², which use the same action (i.e. the tree-level improved SW action corresponding to $c_{\text{sw}} = 1$) for the light quarks, agree when subjected to the same analysis procedure, whereas the Kentucky group results ⁵³, using the unimproved Wilson action ($c_{\text{sw}} = 0$) but with tadpole-improved perturbation theory in the matching, are significantly larger. A similar conclusion is reached by Wittig in ⁴⁴. Because of these uncertainties, as mentioned above, we will not make further use of these results, but will use those obtained with propagating quarks to obtain the value of B_B .

^cIn step (i) of the matching procedure we use $\alpha_V(q^* a)$ evaluated at $q^* = 2.18a^{-1}$ as the strong coupling constant ⁴².

Table 5: Results for the mixing parameter B_B obtained in the quenched approximation using propagating b -quarks. The authors' results for $B_B(\mu)$ at scale μ or for $B_B(m_b)$ with $m_b = 5$ GeV are quoted. They are then scaled to m_b and converted to \hat{B}_B^{nlo} , the renormalization group invariant B parameter. The results may differ slightly from those in the original articles owing to the particular choice of parameters used here: authors' numbers are shown in upright type, numbers produced by us in oblique type.

| | Yr | β | μ/GeV | $B_B(\mu)$ | $B_B(m_b)$ | \hat{B}_B^{nlo} |
|---------------------|----|----------|------------------|------------|------------|--------------------------|
| BBS ⁶⁰ | 97 | ∞ | 2 | 1.02(13) | 0.96(12) | 1.53(19) |
| JLQCD ⁶¹ | 96 | 6.3 | | | 0.840(60) | 1.34(10) |
| JLQCD ⁶¹ | 96 | 6.1 | | | 0.895(47) | 1.42(7) |
| BS ⁹ | 96 | ∞ | 2 | 0.96(6)(4) | 0.90(6)(4) | 1.44(9)(6) |
| ELC ³⁵ | 92 | 6.4 | 3.7 | 0.86(5) | 0.84(5) | 1.34(8) |
| BDHS ³⁹ | 88 | 6.1 | 2 | 1.01(15) | 0.95(14) | 1.51(22) |

3.2 B_B obtained using propagating b -quarks

Calculations with propagating heavy quarks are reported in Table 5. We have scaled all results to a common scale $m_b = 5$ GeV, with the same parameter choice as for the static results above, and then converted both to \hat{B}_B at NLO. The results show no observable dependence on the lattice spacing, although the authors of Ref. ⁶⁰ perform a linear extrapolation to the continuum limit, which is the reason for the relatively large error in the corresponding result. Although the quoted errors are largely statistical, the different groups treat the perturbative matching in different ways, so that it is not appropriate to simply perform a weighted average. Our preferred estimate based on the results in Table 5 is

$$\hat{B}_B^{\text{nlo}} = 1.4(1) . \quad (29)$$

In estimating the error we have assumed that the results are almost independent of the lattice spacing and have not tried to quantify the effects of quenching^d. Calculations to be performed in the near future will use improved actions and operators (reducing the discretization errors to ones which are quadratic in the lattice spacing) and will avoid lattice perturbation theory by using non-perturbative renormalization.

The relevant quantity for B - \bar{B} mixing is $f_B^2 \hat{B}_B$. Taking the result in Eq. (29) above for \hat{B}_B^{nlo} with $f_B = 170(35)$ MeV from Eq. (17) gives

$$f_B \sqrt{\hat{B}_B^{\text{nlo}}} = 201(42) \text{ MeV} \quad (30)$$

^dThe second error in the result from Ref. ⁹ is the authors' estimate of the quenching errors.

as our lattice estimate. An interesting dimensionless quantity is the ratio

$$\xi \equiv \frac{f_{B_s} \sqrt{\hat{B}_{B_s}}}{f_{B_d} \sqrt{\hat{B}_{B_d}}} \quad (31)$$

For propagating quarks, combining the result $f_{B_s}/f_B = 1.14(8)$ from Eq. (20) with $B_{B_s}/B_B = 1.00(3)$ ⁶² gives

$$\xi = 1.14(8). \quad (32)$$

A recent direct extraction of the matrix element $M(\mu)$ gives the ratio $r_{sd} \equiv \xi^2 m_{B_s}^2 / m_{B_d}^2 = 1.54(13)(32)$ ⁶⁰. In the static case, Giménez and Martinelli⁵² find $r_{sd} = 1.43(7)$ by combining $f_{B_s}/f_B = 1.17(3)$ and $B_{B_s}/B_B = 1.01(1)$, and $r_{sd} = 1.35(5)$ from a direct evaluation of the four-quark matrix element measured on the same gauge configurations. The results of the two methods are quite consistent, but future calculations should improve on the precision of r_{sd} .

The above results are largely from quenched calculations. For B_{B_s}/B_B , numerical evidence suggests a small increase on two-flavour dynamical configurations⁹ but the chiral loop estimate^{45,46} is for a decrease of -0.04 in the ratio. We must wait for reliable simulations with dynamical quarks before the size of quenching effects can be determined with confidence.

4 Semileptonic Decays of D and B -mesons

We now discuss semileptonic decays of D and B -mesons, considering in turn the cases in which the c -quark decays into an s - or d -quark and the b -quark decays into a c - or u -quark. The B -meson decay is represented in Figure 5, though the diagram could simply be relabelled to describe the D -meson decay. It is convenient to use space-time symmetries to express the matrix elements in terms of invariant form factors (using the helicity basis for these as defined below). When the final state is a pseudoscalar meson P , parity implies that only the vector component of the $V-A$ weak current contributes to the decay, and there are two independent form factors, f^+ and f^0 , defined by

$$\begin{aligned} \langle P(k) | V^\mu | B(p) \rangle &= f^+(q^2) \left[(p+k)^\mu - \frac{m_B^2 - m_P^2}{q^2} q^\mu \right] \\ &+ f^0(q^2) \frac{m_B^2 - m_P^2}{q^2} q^\mu, \end{aligned} \quad (33)$$

where q is the momentum transfer, $q = p-k$, and $B(p)$ denotes either a B or D meson. When the final-state hadron is a vector meson V , there are four

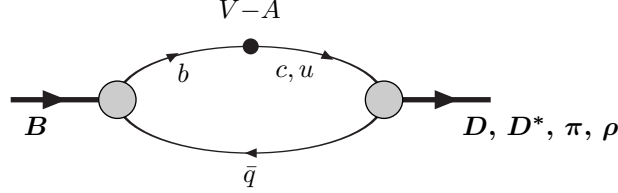


Figure 5: Diagram representing the semileptonic decay of the B -meson. \bar{q} represents the light valence antiquark, and the black circle represents the insertion of the $V-A$ current with the appropriate flavour quantum numbers.

independent form factors:

$$\langle V(k, \varepsilon) | V^\mu | B(p) \rangle = \frac{2V(q^2)}{m_B + m_V} e^{\mu\gamma\delta\beta} \varepsilon_\beta^* p_\gamma k_\delta \quad (34)$$

$$\begin{aligned} \langle V(k, \varepsilon) | A^\mu | B(p) \rangle &= i(m_B + m_V) A_1(q^2) \varepsilon^{*\mu} - i \frac{A_2(q^2)}{m_B + m_V} \varepsilon^* \cdot p (p+k)^\mu \\ &\quad + i \frac{A(q^2)}{q^2} 2m_V \varepsilon^* \cdot p q^\mu, \end{aligned} \quad (35)$$

where ε is the polarization vector of the final-state meson, and $q = p - k$. Below we shall also discuss the form factor A_0 , which is given in terms of those defined above by $A_0 = A + A_3$, with

$$A_3 = \frac{m_B + m_V}{2m_V} A_1 - \frac{m_B - m_V}{2m_V} A_2. \quad (36)$$

4.1 Semileptonic D Decays

The decays $D \rightarrow Kl^+\nu_l$ and $D \rightarrow K^*l^+\nu_l$ provide a good test for lattice calculations since the relevant CKM matrix element V_{cs} is well constrained in the standard model. The form factors for the decays $D \rightarrow \pi l^+\nu_l$ and $D \rightarrow \rho l^+\nu_l$ can also be computed in lattice simulations. As explained in the introduction, charm quarks are light enough to be simulated directly (though one still needs to be wary of mass-dependent discretization errors). Furthermore, strange quarks can also be simulated directly, so for $D \rightarrow K$ or K^* decays there is only one quark for which a chiral extrapolation needs to be performed. For semileptonic D -meson decays the whole physical phase space can be sampled^e,

^eIn addition, one obtains the form factors for unphysical, negative, values of q^2 .

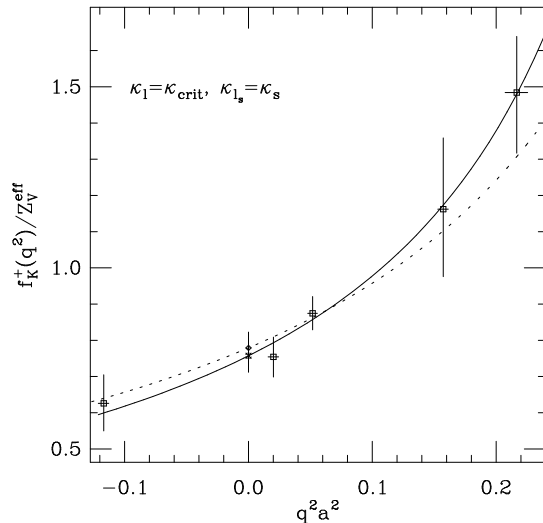


Figure 6: UKQCD lattice results for the form factor $f^+(q^2)$ in semileptonic $D \rightarrow K$ decay⁶³. The form factor is plotted as a function of the dimensionless variable $q^2 a^2$ and before multiplication by the appropriate lattice-to-continuum normalization factor Z_V^{eff} . The label $\kappa_l = \kappa_{\text{crit}}, \kappa_s = \kappa_s$ shows that the light quark masses have been extrapolated to give the physical $D \rightarrow K$ form factor. The curves show fits of pole dominance behaviour to the data: the solid line is a two parameter fit, the dashed line a fit where the pole mass is fixed to the corresponding 1^- vector meson mass determined in the same lattice calculation. The cross and diamond show the interpolations of the fits to $q^2 = 0$.

while keeping the spatial momenta of the initial and final state mesons small in order to minimise the momentum-dependent discretization errors.

Although the lattice calculations actually measure the q^2 dependence of the form factors, as shown by the example of f^+ for the $D \rightarrow K$ decay in Figure 6⁶³, we follow the standard practice of quoting values at $q^2 = 0$. In contrast to the case for B decays to be discussed below, we emphasise that this involves an interpolation and so is relatively well controlled. We refer the reader to the original papers for detailed discussions of the q^2 -dependence of the form factors.

Lattice results for the $D \rightarrow K^{(*)}$ form factors are collected in Table 6 and illustrated in Figure 7, while results for the $D \rightarrow \pi, \rho$ form factors appear in Table 7. These are all from quenched simulations and no group has performed a continuum extrapolation. Our summary view of these results is obtained by considering the more recent results from WUP⁶⁴, LANL^{65,66}, UKQCD⁶³ and APE⁶⁷ which all use either the improved SW action or the Wilson action

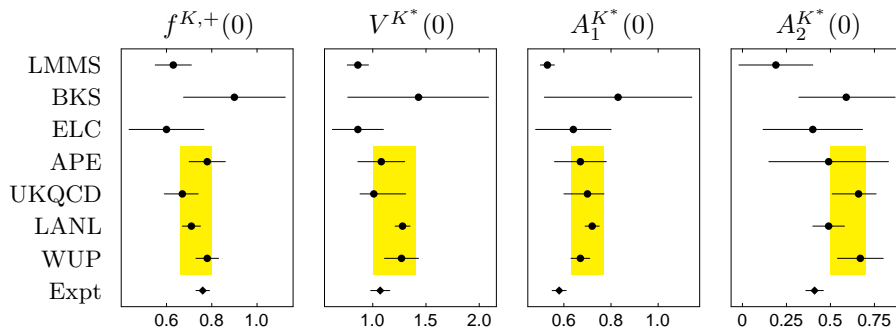


Figure 7: Lattice results for $D \rightarrow K$ and $D \rightarrow K^*$ semileptonic decay form factors at zero momentum transfer, and comparison with experimental results from the survey in Ref. ⁶⁸. The shaded bands show our summary values, indicating which results they are based on, as discussed in the text.

with a KLM normalization. The summary values are presented in Table 8, along with recent experimental world averages ⁶⁸ in the $D \rightarrow K, K^*$ case. The values quoted reflect the fact that f^+ and A_1 are the best measured while the $D \rightarrow \pi, \rho$ form factors are smaller with slightly larger errors. The shaded bands in Figure 7 show our estimates in the $D \rightarrow K, K^*$ case and indicate which results they are based on.

One sees that the lattice and experimental results agree rather well. The lattice values for A_1 and A_2 are both high compared to experiment: however, these depend on the correct normalization of the lattice axial vector current which is less well known than the vector current normalization needed for f^+ and V . In particular, the non-degeneracy of the c - and s -quarks means that there is no natural normalization condition to use for the weak current. This contrasts with the situation for heavy-to-heavy semileptonic decays, described in Section 4.2, where one can make use of the conservation of the vector current of degenerate quarks.

4.2 Semileptonic $B \rightarrow D$ and $B \rightarrow D^*$ Decays

Semileptonic $B \rightarrow D^*$ and, more recently, $B \rightarrow D$ decays are used to determine the V_{cb} element of the CKM matrix. Heavy quark symmetry is rather powerful in controlling the theoretical description of these heavy-to-heavy quark transitions, as described by Neubert in the chapter on “ B Decays and the Heavy Quark Expansion” in this volume ⁷². In describing lattice results for these decays, we will quote theoretical results and direct the reader to Ref. ⁷² for

Table 6: Collected lattice results for $D \rightarrow K, K^*$ semileptonic decay form factors at $q^2 = 0$.

| | Yr | $f^+(0)$ | $f^0(0)$ | $V(0)$ | V/A_1 |
|-----------------------|-------|-----------------------|-------------|-----------------------------|-----------------------------|
| WUP ⁶⁴ | 97 | 0.78(5) | 0.78(5) | 1.27(16) | |
| LANL ^{65,66} | 95–96 | 0.71(4) | 0.73(3) | 1.28(7) | 1.78(7) |
| UKQCD ⁶³ | 95 | 0.67($\frac{7}{8}$) | 0.65(7) | 1.01($\frac{30}{13}$) | 1.4($\frac{5}{2}$) |
| APE ⁶⁷ | 95 | 0.78(8) | | 1.08(22) | 1.6(3) |
| ELC ⁶⁹ | 94 | 0.60(15)(7) | | 0.86(24) | 1.3(2) |
| BKS ⁷⁰ | 91–92 | 0.90(8)(21) | 0.70(8)(24) | 1.43(45)($\frac{48}{19}$) | 1.99(22)($\frac{31}{35}$) |
| LMMS ⁷¹ | 89–92 | 0.63(8) | | 0.86(10) | 1.6(2) |

| | Yr | $A_1(0)$ | $A_2(0)$ | A_2/A_1 | $A_0(0)$ |
|-----------------------|-------|-------------------------|-----------------------------|-----------------------------|------------------------|
| WUP ⁶⁴ | 97 | 0.67(4) | 0.67(13) | | |
| LANL ^{65,66} | 95–96 | 0.72(3) | 0.49(9) | 0.68(11) | 0.84(3) |
| UKQCD ⁶³ | 95 | 0.70($\frac{10}{10}$) | 0.66($\frac{10}{15}$) | 0.9(2) | 0.75($\frac{5}{11}$) |
| APE ⁶⁷ | 95 | 0.67(11) | 0.49(34) | 0.7(4) | |
| ELC ⁶⁹ | 94 | 0.64(16) | 0.40(28)(4) | 0.6(3) | |
| BKS ⁷⁰ | 91–92 | 0.83(14)(28) | 0.59(14)($\frac{24}{23}$) | 0.70(16)($\frac{20}{15}$) | 0.71(16)(25) |
| LMMS ⁷¹ | 89–92 | 0.53(3) | 0.19(21) | 0.4(4) | |

Table 7: Collected lattice results for $D \rightarrow \pi, \rho$ semileptonic decay form factors at $q^2 = 0$.

| | Yr | $f^+(0)$ | $f^0(0)$ | $V(0)$ | V/A_1 |
|---------------------|-------|-------------------------|-------------------------|-------------------------|--------------|
| WUP ⁶⁴ | 97 | 0.73(6) | 0.73(6) | 1.18(17) | |
| LANL ⁶⁵ | 95 | 0.56(8) | 0.62(5) | 1.18(15) | 1.77(16) |
| UKQCD ⁶³ | 95 | 0.61($\frac{12}{11}$) | 0.53($\frac{12}{11}$) | 0.95($\frac{29}{14}$) | |
| BKS ⁷⁰ | 91–92 | 0.84(12)(35) | 0.62(6)(34) | 1.07(49)(35) | 2.01(40)(32) |
| LMMS ⁷¹ | 89–92 | 0.58(9) | | 0.78(12) | |

| | Yr | $A_1(0)$ | $A_2(0)$ | A_2/A_1 | $A_0(0)$ |
|---------------------|-------|-----------------------------|-----------------------------|-----------------------------|------------------------|
| WUP ⁶⁴ | 97 | 0.63(5) | 0.64(14) | | |
| LANL ⁶⁵ | 95 | 0.67(7) | 0.44(24) | 0.67(31) | |
| UKQCD ⁶³ | 95 | 0.63($\frac{6}{9}$) | 0.51($\frac{10}{15}$) | | 0.70($\frac{5}{12}$) |
| BKS ⁷⁰ | 91–92 | 0.65(15)($\frac{24}{23}$) | 0.59(31)($\frac{28}{25}$) | 0.89(37)($\frac{22}{19}$) | 0.64(17)(21) |
| LMMS ⁷¹ | 89–92 | 0.45(4) | 0.02(26) | | |

Table 8: Summary of lattice and experimental results for $D \rightarrow K, K^*$ and $D \rightarrow \pi, \rho$ semileptonic decay form factors at $q^2 = 0$. The experimental numbers are taken from the survey in Ref. ⁶⁸.

| | $D \rightarrow K, K^*$ | | $D \rightarrow \pi, \rho$ |
|----------|------------------------|---------|---------------------------|
| | lattice | expt | lattice |
| $f^+(0)$ | 0.73(7) | 0.76(3) | 0.65(10) |
| $V(0)$ | 1.2(2) | 1.07(9) | 1.1(2) |
| $A_1(0)$ | 0.70(7) | 0.58(3) | 0.65(7) |
| $A_2(0)$ | 0.6(1) | 0.41(5) | 0.55(10) |

details and references.

In the heavy quark limit all six form factors in Eqs. (33–35) are related and there is just one universal form factor $\xi(\omega)$, known as the Isgur–Wise (IW) function which contains all the non-perturbative QCD effects. Specifically:

$$\begin{aligned}
 f^+(q^2) &= V(q^2) = A_0(q^2) = A_2(q^2) \\
 &= \left[1 - \frac{q^2}{(m_B + m_D)^2} \right]^{-1} A_1(q^2) = \frac{m_B + m_D}{2\sqrt{m_B m_D}} \xi(\omega), \quad (37)
 \end{aligned}$$

where $\omega = v_B \cdot v_D$ is the velocity transfer variable. Here the label D represents the D - or D^* -meson as appropriate (pseudoscalar and vector mesons are degenerate in this leading approximation). Vector current conservation implies that the IW-function is normalized at zero recoil, i.e. that $\xi(1) = 1$. This property is particularly important in the extraction of V_{cb} .

The relations in Eq. (37) are valid up to perturbative and power corrections. Allowing for corrections to the heavy quark limit, one writes the decay distribution for $B \rightarrow D^*$ as

$$\begin{aligned}
 \frac{d\Gamma}{d\omega} &= \frac{G_F^2}{48\pi^3} (m_B - m_{D^*})^2 m_{D^*}^3 \sqrt{\omega^2 - 1} (\omega + 1)^2 \\
 &\times \left[1 + \frac{4\omega}{\omega + 1} \frac{m_B^2 - 2\omega m_B m_{D^*} + m_{D^*}^2}{(m_B - m_{D^*})^2} \right] |V_{cb}|^2 \mathcal{F}^2(\omega), \quad (38)
 \end{aligned}$$

where $\mathcal{F}(\omega)$ is the “physical form factor” given by the IW-function combined with perturbative and power corrections. To extract $|V_{cb}|$ one extrapolates measurements of the product $\mathcal{F}(\omega)|V_{cb}|$ to the zero-recoil point, $\omega = 1$, and uses a theoretical evaluation of the normalization $\mathcal{F}(1)$ ⁷².

A theoretical understanding of the shape of the physical form factor would be useful to guide the extrapolation of the experimental data, which currently

show rather a wide variation for the slope and intercept^{72,73}, and also as a test of our understanding of the QCD effects. We expand \mathcal{F} as a power series in $\omega - 1$:

$$\mathcal{F}(\omega) = \mathcal{F}(1) [1 - \hat{\rho}^2(\omega - 1) + \hat{c}(\omega - 1)^2 + \dots]. \quad (39)$$

The slope parameter $\hat{\rho}^2$ differs from the slope parameter ρ^2 of the IW function itself by heavy quark symmetry violating corrections⁷²,

$$\hat{\rho}^2 = \rho^2 + (0.16 \pm 0.02) + \text{power corrections}. \quad (40)$$

To discuss lattice results for the shape of the IW function, and to search for corrections to the relations obtained using heavy quark symmetry, it is convenient to work with the following set of form factors (expressed in terms of four-velocities) which in the heavy quark limit either vanish or are equal to the IW function:

$$\begin{aligned} \frac{\langle D(v') | \bar{c} \gamma^\mu b | B(v) \rangle}{\sqrt{m_B m_D}} &= (v+v')^\mu h_+(\omega) + (v-v')^\mu h_-(\omega) \\ \frac{\langle D^*(v') | \bar{c} \gamma^\mu b | B(v) \rangle}{\sqrt{m_B m_D}} &= i \epsilon^{\mu\nu\alpha\beta} \epsilon_\nu^* v'_\alpha v_\beta h_V(\omega) \\ \frac{\langle D^*(v') | \bar{c} \gamma^\mu \gamma_5 b | B(v) \rangle}{\sqrt{m_B m_D}} &= (\omega+1) \epsilon^{*\mu} h_{A_1}(\omega) - \epsilon^{* \cdot} v (v^\mu h_{A_2}(\omega) + v'^\mu h_{A_3}(\omega)) \end{aligned}$$

where

$$h_i(\omega) = (\alpha_i + \beta_i(\omega) + \gamma_i(\omega)) \xi(\omega) \quad (41)$$

with

$$\alpha_+ = \alpha_V = \alpha_{A_1} = \alpha_{A_3} = 1, \quad \alpha_- = \alpha_{A_2} = 0. \quad (42)$$

The β_i and γ_i denote perturbative and power corrections (in $1/m_{b,c}$) respectively. The statement of Luke's theorem⁷⁴ is

$$\gamma_{+,A_1}(1) = O(\Lambda_{\text{QCD}}^2/m_{c,b}^2). \quad (43)$$

The principal difficulty for lattice calculations is to separate the physical heavy quark mass dependence due to power corrections from the unphysical one due to mass-dependent discretization errors. One must also address the question of lattice-to-continuum matching. We will illustrate our discussion using the analysis procedure applied by the UKQCD collaboration⁷⁵ (who use the SW action for all quarks so that the leading mass-dependent discretization errors are formally reduced to $O(\alpha_s m_Q a)$ and $O(m_Q^2 a^2)$). Consider the case of h_+ . For this form factor we have the protection of Luke's theorem at zero recoil

Table 9: Values of the Slope of the IW-function of a heavy meson, obtained using lattice QCD. The table indicates which functional form from Eq. (47) has been fitted to and which form factor has been used in the extraction. The systematic error in the UKQCD results incorporates the variation from fitting to all functional forms in Eq. (47). BSS note that $\rho_{u,d}^2$ is 12% smaller than ρ_s^2 , but do not quote a separate result.

| | Yr | $\rho_{u,d}^2$ | ρ_s^2 | fit | using |
|---------------------|----|---------------------------------|---------------------------------|-----|-----------|
| LANL ⁶⁶ | 96 | 0.97(6) | | NR | h_+ |
| UKQCD ⁷⁵ | 95 | $0.9(\frac{2}{3})(\frac{4}{2})$ | $1.2(\frac{2}{2})(\frac{2}{1})$ | NR | h_+ |
| UKQCD ⁷⁶ | 94 | $0.9(\frac{4}{5})(\frac{9}{1})$ | $1.2(\frac{3}{3})(\frac{7}{1})$ | NR | h_{A_1} |
| BSS ⁷⁷ | 93 | | 1.24(26)(36) | lin | h_+ |
| BSS ⁷⁷ | 93 | | 1.41(19)(41) | NR | h_+ |

and, for degenerate ($Q = Q'$) transitions, conservation of the vector current $\bar{Q}\gamma_\mu Q$ provides the further constraints:

$$\beta_+(1; m_Q, m_Q) = 0, \quad \gamma_+(1; m_Q, m_Q) = 0. \quad (44)$$

The correct normalization of the vector current can be assured by requiring that the electric charge of the meson be 1. We therefore define the continuum form factor by,

$$h_+(\omega; m_Q, m_{Q'}) \equiv (1 + \beta_+(1; m_Q, m_{Q'})) \frac{h_+^L(\omega; m_Q, m_{Q'})}{h_+^L(1; m_Q, m_{Q'})}, \quad (45)$$

where $h_i^L(\omega; m_Q, m_{Q'})$ is the (un-normalized) form factor calculated directly in the lattice simulation. This definition partially removes discretization errors and also removes ω -independent power corrections while maintaining the known normalization conditions. If the remaining power corrections are small, then

$$\frac{h_+(\omega)}{1 + \beta_+(\omega)} \quad (46)$$

is effectively the IW function, $\xi(\omega)$. This is convenient for extracting $\xi(\omega)$, but the definition of Eq. (45) precludes a determination of the zero-recoil power corrections. These corrections should be small, being suppressed by two powers of the heavy quark mass. However, applying an analogous procedure to the $h_{A_1}(\omega)$ form factor relevant for $B \rightarrow D^*$ decays will not allow the $1/m_c^2$ corrections to $\mathcal{F}(1)$, one of the dominant theoretical uncertainties, to be determined.

UKQCD confirm⁷⁵ that their results for $h_+/(1 + \beta_+)$ are indeed independent of the heavy quark masses and hence demonstrate, within the available

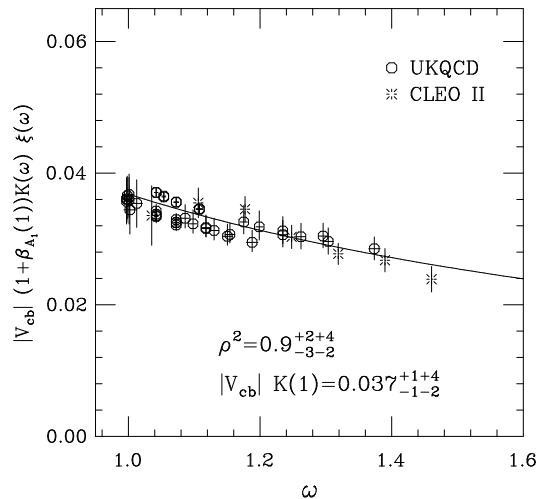


Figure 8: Fit of the UKQCD lattice results for $|V_{cb}|\mathcal{F}(\omega)$ ⁷⁵ to the experimental data from the CLEO collaboration⁷⁸.

precision, that there *is* an IW function. Moreover, a similar analysis for the h_{A_1} form factor reveals the same function⁷⁶, so the IW function appears indeed to be universal. Performing extrapolations to the light (u -, d -) and strange (s -) quark masses and fitting to

$$\xi(\omega) = \begin{cases} \xi_{\text{NR}}(\omega) \equiv \frac{2}{\omega+1} \exp(-2(\rho^2-1)\frac{\omega-1}{\omega+1}) & \text{NR} \\ 1 - \rho^2(\omega-1) & \text{linear} \\ 1 - \rho^2(\omega-1) + \frac{c}{2}(\omega-1)^2 & \text{quadratic} \end{cases} \quad (47)$$

gives lattice determinations of the slope of the IW function, as listed in Table 9. Since ‘the’ IW function is different for different light degrees of freedom, the results in the table are labelled with subscripts u , d or s as appropriate.

In Figure 8 we show the comparison of the UKQCD lattice results⁷⁵ with $B \rightarrow D^*$ data (in 1995) from the CLEO collaboration⁷⁸. A chi-squared fit is made to the experimental data for $|V_{cb}|[1 + \beta_{A_1}(1)]K(\omega)\xi_{u,d}(\omega) \equiv |V_{cb}|\mathcal{F}(\omega)$. $K(\omega)$ incorporates radiative corrections away from zero-recoil ($\beta_{A_1}(\omega)$), non-perturbative power corrections ($\gamma_{A_1}(\omega)$) and the contributions of the other form factors to the rate. The current lattice calculations cannot distinguish the ω dependence of $K(\omega)$, so it is taken to be a constant and hence $\rho_{u,d}^2$ and $\hat{\rho}^2$ are not distinguished. The slope of the IW function is constrained to the lattice result in the fit so that the only free parameter is $|V_{cb}|\mathcal{F}(1)$. The result

of the fit is ⁷⁵

$$|V_{cb}| \mathcal{F}(1) = 0.037^{+1}_{-1} {}^{+2}_{-2} {}^{+4}_{-4}. \quad (48)$$

We should also mention $B \rightarrow D$ semileptonic decays, which are beginning to be measured experimentally ^{79,73} with good precision, despite the helicity suppression in $d\Gamma(B \rightarrow D l \bar{\nu}_l)/d\omega$. The differential decay rate depends on both $h_+(\omega)$ and $h_-(\omega)$. However, h_- is rather poorly determined to date in lattice calculations, so that it is difficult to evaluate the $O(1/m_Q)$ corrections.

Direct lattice calculations of the IW function are being undertaken using discretizations of the heavy quark effective theory ^{80–83}. These studies are very interesting, but the results are not yet useful for phenomenology. An interesting theoretical feature of this approach is the formulation of the HQET at non-zero velocity in Euclidean space ^{84–86}.

Finally we note that a first lattice study of the semileptonic decays $\Lambda_b \rightarrow \Lambda_c l \nu$ and $\Xi_b \rightarrow \Xi_c l \nu$ has recently been performed ⁸⁷, giving predictions for the decay distributions and the baryonic Isgur-Wise function. We refer the interested reader to Ref. ⁸⁷ for details.

4.3 Semileptonic $B \rightarrow \rho$ and $B \rightarrow \pi$ Decays and the Rare Decay $\bar{B} \rightarrow K^* \gamma$

In this subsection we consider the heavy-to-light semileptonic decays $B \rightarrow \rho$ and $B \rightarrow \pi$ which are now being used experimentally to determine the V_{ub} matrix element ^{73,88}. Several groups have evaluated form factors for these decays using lattice simulations ^{69,67,64,89–91} (see the recent review in ¹¹). We will also consider the rare radiative decay $\bar{B} \rightarrow K^* \gamma$ which is related by heavy quark and light flavour symmetries to the $B \rightarrow \rho$ semileptonic decay, and which was observed experimentally for the first time in 1993 ^{92,93}.

Form factors for semileptonic $B \rightarrow \pi$ decays were defined above in Eq. (33) and for $B \rightarrow \rho$ decays in Eq. (35). For completeness, we define here form factors for the matrix element of the magnetic moment operator responsible for the short distance contribution to the $\bar{B} \rightarrow K^* \gamma$ decay:

$$\langle K^*(k, \varepsilon) | \bar{s} \sigma_{\mu\nu} q^\nu b_R | B(p) \rangle = \sum_{i=1}^3 C_\mu^i T_i(q^2), \quad (49)$$

where $q = p - k$, ε is the polarization vector of the K^* and

$$C_\mu^1 = 2\varepsilon_{\mu\nu\lambda\rho} \varepsilon^{*\nu} p^\lambda k^\rho, \quad (50)$$

$$C_\mu^2 = \varepsilon_\mu^* (m_B^2 - m_{K^*}^2) - \varepsilon \cdot q (p + k)_\mu, \quad (51)$$

$$C_\mu^3 = \varepsilon^* \cdot q \left(q_\mu - \frac{q^2}{m_B^2 - m_{K^*}^2} (p + k)_\mu \right). \quad (52)$$

Table 10: Leading M dependence of form factors for heavy-to-light decays in the helicity basis. The dependence follows from heavy quark symmetry applied at *fixed* velocity transfer ω . Note that only three of the four A_i form factors for $B \rightarrow \rho l \nu$ are independent.

| form factor | t -channel exchange | leading M dependence | form factor | t -channel exchange | leading M dependence |
|----------------------------|-----------------------|------------------------|----------------------------|-----------------------|------------------------|
| $B \rightarrow \rho l \nu$ | | | $B \rightarrow \pi l \nu$ | | |
| V | 1^- | $M^{1/2}$ | f^+ | 1^- | $M^{1/2}$ |
| A_1 | 1^+ | $M^{-1/2}$ | f^0 | 0^+ | $M^{-1/2}$ |
| A_2 | 1^+ | $M^{1/2}$ | $B \rightarrow K^* \gamma$ | | |
| A_3 | 1^+ | $M^{3/2}$ | T_1 | 1^- | $M^{1/2}$ |
| A_0 | 0^- | $M^{1/2}$ | T_2 | 1^+ | $M^{-1/2}$ |

T_3 does not contribute to the physical $\bar{B} \rightarrow K^* \gamma$ amplitude for which $q^2 = 0$, and $T_1(0)$ and $T_2(0)$ are related by,

$$T_1(q^2=0) = iT_2(q^2=0). \quad (53)$$

Hence, for the process $\bar{B} \rightarrow K^* \gamma$, we need to determine T_1 and/or T_2 at the on-shell point $q^2=0$.

Heavy quark symmetry is less predictive for heavy-to-light decays than for heavy-to-heavy ones. In particular, there is no normalization condition at zero recoil corresponding to the condition $\xi(1) = 1$, which is so useful in the extraction of V_{cb} . The lack of such a condition puts a premium on the results from nonperturbative calculational techniques, such as lattice QCD. Heavy quark symmetry does, however, give useful scaling laws for the behaviour of the form factors with the mass of the heavy quark at fixed ω . Moreover, the heavy quark spin symmetry relates the $B \rightarrow V$ matrix elements^{94,95} (where V is a light vector particle) of the weak current and magnetic moment operators, thereby relating the amplitudes for the two processes $\bar{B}^0 \rightarrow \rho^+ l^- \bar{\nu}_l$ and $\bar{B} \rightarrow K^* \gamma$, up to $SU(3)$ flavour symmetry breaking effects.

For fixed ω the scaling laws for the form factors given by heavy quark symmetry are as follows:

$$f(q^2(\omega))|_{\omega \text{ fixed}} \Theta = M^{\nu_f} \gamma_f \left(1 + \frac{\delta_f}{M} + \frac{\epsilon_f}{M^2} + \dots \right) \quad (54)$$

where f labels the form factor, M is the mass of the heavy-light meson and Θ is a calculable leading logarithmic correction. The leading M dependences, M^{ν_f} , are listed in Table 10. Lattice calculations with propagating quarks use a range of quark masses around the charm mass and generally employ these

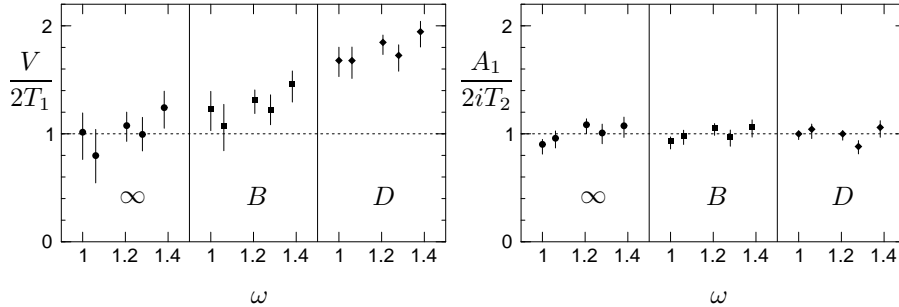


Figure 9: Ratios $V/2T_1$ and $A_1/2iT_2$ for five values of ω at three different heavy-light pseudoscalar masses, around the D mass, around the B mass and in the infinite mass limit. The horizontal dashed line denotes the heavy quark symmetry prediction in the infinite mass limit. Data from Ref. ⁹⁰.

scaling relations to extrapolate to the B mass: this is the case for results from ELC, APE and UKQCD. In the limit $M \rightarrow \infty$ we also have the relations

$$A_1(q^2(\omega)) = 2iT_2(q^2(\omega)), \quad V(q^2(\omega)) = 2T_1(q^2(\omega)), \quad (55)$$

at fixed ω . The UKQCD collaboration have checked the validity of the relations in Eq. (55) ⁹⁰, finding that they are well satisfied in the infinite mass limit as shown in Figure 9. However, the ratio $V/2T_1$ already shows significant deviations from the limiting value, 1, at the B mass.

There are also kinematic constraints on the form factors at $q^2 = 0$:

$$f^+(0) = f^0(0), \quad T_1(0) = iT_2(0), \quad A_0(0) = A_3(0), \quad (56)$$

which will be useful below.

From lattice simulations we can obtain the form factors only for part of the physical phase space. In order to control discretization errors we require that the three-momenta of the B , π and ρ mesons be small in lattice units. This implies that we determine the form factors at large values of momentum transfer $q^2 = (p_B - p_{\pi,\rho})^2$. Experiments can already reconstruct exclusive semileptonic $b \rightarrow u$ decays (see, for example, the review in ⁸⁸) and as techniques improve and new facilities begin operation, we can expect to be able to compare the lattice form factor calculations directly with experimental data at large q^2 . A proposal in this direction was made by UKQCD ⁹⁰ for $\bar{B}^0 \rightarrow \rho^+ l^- \bar{\nu}_l$ decays. To get some idea of the precision that might be reached, they parametrize the differential decay rate distribution near q_{\max}^2 by:

$$\frac{d\Gamma(\bar{B}^0 \rightarrow \rho^+ l^- \bar{\nu}_l)}{dq^2} = 10^{-12} \frac{G_F^2 |V_{ub}|^2}{192\pi^3 M_B^3} q^2 \lambda^{\frac{1}{2}}(q^2) a^2 (1 + b(q^2 - q_{\max}^2)), \quad (57)$$

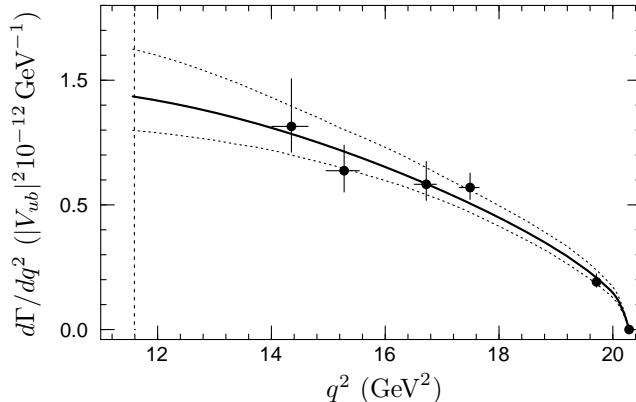


Figure 10: Differential decay rate as a function of q^2 for the semileptonic decay $\bar{B}^0 \rightarrow \rho^+ l^- \bar{\nu}_l$, taken from⁹⁰. Points are measured lattice data, solid curve is fit from Eq. (57) with parameters given in Eq. (58). The dashed curves show the variation from the statistical errors in the fit parameters. The vertical dotted line marks the charm endpoint.

where a and b are parameters, and the phase-space factor λ is given by $\lambda(q^2) = (m_B^2 + m_\rho^2 - q^2)^2 - 4m_B^2 m_\rho^2$. The constant a plays the role of the IW function evaluated at $\omega = 1$ for heavy-to-heavy transitions, but in this case there is no symmetry to determine its value at leading order in the heavy quark effective theory. UKQCD obtain⁹⁰

$$\begin{aligned} a &= 4.6 \pm_{0.3}^{0.4} \pm 0.6 \text{ GeV}, \\ b &= (-8 \pm_6^4) \times 10^{-2} \text{ GeV}^2. \end{aligned} \quad (58)$$

The fits are less sensitive to b , so it is less well-determined. The result for a incorporates a systematic error dominated by the uncertainty ascribed to discretization errors and would lead to an extraction of $|V_{ub}|$ with less than 10% statistical error and about 12% systematic error from the theoretical input. The prediction for the $d\Gamma/dq^2$ distribution based on these numbers is presented in Figure 10. With sufficient experimental data an accurate lattice result at a single value of q^2 would be sufficient to fix $|V_{ub}|$.

In principle, a similar analysis could be applied to the decay $\bar{B}^0 \rightarrow \pi^+ l^- \bar{\nu}_l$. However, UKQCD find that the difficulty of performing the chiral extrapolation to a realistically light pion from the unphysical pions used in the simulations makes the results less certain. The $B \rightarrow \pi$ decay also has a smaller fraction of events at high q^2 , so it will be more difficult experimentally to extract sufficient data in this region for a detailed comparison.

We would also like to know the full q^2 dependence of the form factors,

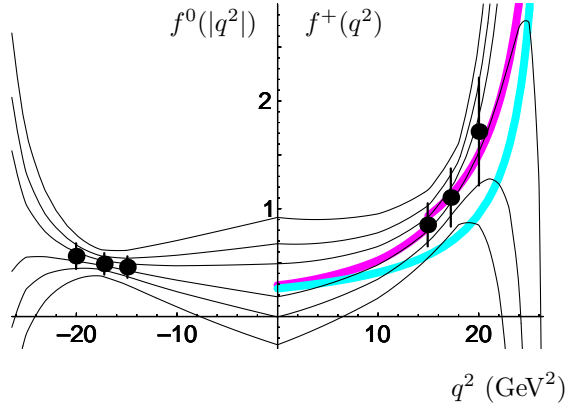


Figure 11: Bounds on f^+ and f^0 for $\bar{B}^0 \rightarrow \pi^+ l^- \bar{\nu}_l$ from dispersive constraints⁹⁶. The data points are from UKQCD⁸⁹, with added systematic errors. The pairs of fine curves are, outermost to innermost, 95%, 70% and 30% bounds. The upper and lower shaded curves are light-cone⁹⁸ and three-point⁹⁹ sum rule results respectively.

which involves a large extrapolation in q^2 from the high values where lattice calculations produce results, down to $q^2 = 0$. In particular the radiative decay $\bar{B} \rightarrow K^* \gamma$ occurs at $q^2 = 0$, so that existing lattice simulations cannot make a direct calculation of the necessary form factors.

An interesting approach to this extrapolation problem has been applied by Lellouch⁹⁶ for $\bar{B}^0 \rightarrow \pi^+ l^- \bar{\nu}_l$. Using dispersion relations constrained by UKQCD lattice results at large values of q^2 and kinematical constraints at $q^2 = 0$, one can tighten the bounds on form factors at all values of q^2 . This technique relies on perturbative QCD in evaluating one side of the dispersion relations, together with general properties of field theory, such as unitarity, analyticity and crossing. It provides model-independent results which are illustrated in Figure 11. The results (at 50% CL — see Ref.⁹⁶ for details) are

$$f^+(0) = 0.10-0.57, \quad (59)$$

$$\Gamma(\bar{B}^0 \rightarrow \pi^+ l^- \bar{\nu}_l) = 4.4-13 |V_{ub}^2| \text{ps}^{-1}. \quad (60)$$

Unfortunately these bounds are not very restrictive when constrained by existing lattice data. In principle, this method can be applied to $B \rightarrow \rho$ decays also, but is more complicated there, and the calculations have yet to be performed. Recently, Becirevic⁹⁷ has applied the method for $\bar{B} \rightarrow K^* \gamma$, using APE lattice results as constraints. However, he has not applied the kinematic constraint from Eq. (56) and the resulting bounds are not informative: they become so,

Table 11: Lattice results for $\bar{B}^0 \rightarrow \pi^+ l^- \bar{\nu}_l$ using various ansätze for the form factor f^+ . The decay rates are values for $\Gamma(\bar{B}^0 \rightarrow \pi^+ l^- \bar{\nu}_l)/|V_{ub}|^2 \text{ps}^{-1}$. ELC⁶⁹ and APE⁶⁷ results are from their method ‘b’, which uses the heavy quark scaling laws of Eq. (54) to extrapolate from D - to B -mesons at fixed ω .

| | Yr | β | c_{sw} | norm | Rate | $f^+(0)$ |
|---------------------|----|---------|-----------------|------|---------------------|-------------|
| UKQCD ⁹¹ | 97 | 6.2 | 1 | rel | $8.5^{(33)}_{(14)}$ | 0.27(11) |
| WUP ⁶⁴ | 97 | 6.3 | 0 | nr | | 0.43(19) |
| APE ⁶⁷ | 95 | 6.0 | 1 | rel | 8 ± 4 | 0.35(8) |
| ELC ⁶⁹ | 94 | 6.4 | 0 | rel | 9 ± 6 | 0.30(14)(5) |

however, once he uses a light-cone sum rule evaluation of $T_1(0) = iT_2(0)$ as an additional constraint. These dispersive methods can be used with other approaches in addition to lattice results and sum rules, such as quark models, or even in direct comparisons with experimental data, to check for compatibility with QCD and to extend the range of results.

For now we must rely on model input to guide q^2 extrapolations. We can ensure that any assumed q^2 -dependence of the form factors is consistent with the requirements imposed by heavy quark symmetry, as shown in Eq. (54), together with the kinematical relations of Eq. (56). Even with these constraints, however, current lattice data do not by themselves distinguish a preferred q^2 -dependence. Fortunately, more guidance is available from light-cone sum rule analyses^{100,101} which lead to scaling laws for the form factors at fixed (low) q^2 rather than at fixed ω as in Eq. (54). In particular all form factors scale like $M^{-3/2}$ at $q^2 = 0$:

$$f(0)\Theta = M^{-3/2}\gamma_f \left(1 + \frac{\delta_f}{M} + \frac{\epsilon_f}{M^2} + \dots \right). \quad (61)$$

It is therefore important to use ansätze for the form factors compatible with as many of the known constraints as possible.

Lattice results for $\bar{B}^0 \rightarrow \pi^+ l^- \bar{\nu}_l$, $\bar{B}^0 \rightarrow \rho^+ l^- \bar{\nu}_l$ and $\bar{B} \rightarrow K^* \gamma$ are reported in Tables 11, 12 and 13 respectively. ELC⁶⁹ and APE⁶⁷ fit lattice data for the semileptonic decays at a single value of q^2 to a simple pole form with the appropriate pole mass also determined by their data. For the f^0 and A_1 form factors, this is consistent with heavy quark symmetry requirements, kinematic relations and light-cone scaling relations at $q^2 = 0$, Eq. (61), but for the other form factors it is not simultaneously consistent. The WUP⁶⁴ results are found by scaling form factors at $q^2 = 0$ from results with quark masses around the charm mass to the b -quark mass. However, the scaling laws used do not follow the light-cone scaling relations of Eq. (61).

Table 12: $\bar{B}^0 \rightarrow \rho^+ l^- \bar{\nu}_l$ results from lattice simulations. The decay rates are values for $\Gamma(\bar{B}^0 \rightarrow \rho^+ l^- \bar{\nu}_l)/|V_{ub}|^2 \text{ps}^{-1}$. ELC⁶⁹ and APE⁶⁷ results are from their method ‘b’, which uses the heavy quark scaling laws of Eq. (54) to extrapolate from D - to B -mesons at fixed ω .

| | Yr | β | c_{sw} | norm | Rate | $V(0)$ | $A_1(0)$ | $A_2(0)$ |
|---------------------|----|---------|-----------------|------|----------------------|----------------|----------------|----------------|
| UKQCD ⁹¹ | 97 | 6.2 | 1 | rel | 16.5($^{35}_{33}$) | 0.35(6_5) | 0.27(5_4) | 0.26(5_3) |
| WUP ⁶⁴ | 97 | 6.3 | 0 | nr | | 0.65(15) | 0.28(3) | 0.46(23) |
| APE ⁶⁷ | 95 | 6.0 | 1 | rel | 12 ± 6 | 0.53(31) | 0.24(12) | 0.27(80) |
| ELC ⁶⁹ | 94 | 6.4 | 0 | rel | 14 ± 12 | 0.37(11) | 0.22(5) | 0.49(21)(5) |

The latest UKQCD study⁹¹ uses models consistent with all constraints, including the light-cone sum rule scaling relations^f. For $\bar{B}^0 \rightarrow \pi^+ l^- \bar{\nu}_l$ UKQCD use a dipole(pole) model for $f^+(f^0)$, while for $\bar{B}^0 \rightarrow \rho^+ l^- \bar{\nu}_l$ and $\bar{B} \rightarrow K^* \gamma$ (collectively denoted by $B \rightarrow V$) they use a model inspired by Stech¹⁰² which expresses *all* the form factors for the semileptonic and radiative decays of a heavy pseudoscalar meson to a light vector meson in terms of a single function, taken to be a simple pole form for A_1 . In lattice calculations one has the freedom to adjust hadron masses by tuning the quark masses used in the simulation. UKQCD use this freedom to perform a combined fit within their model for all the $B \rightarrow V$ form factors simultaneously, first with $V = \rho$ and then with $V = K^*$. From the first fit they obtain the form factors for $\bar{B}^0 \rightarrow \rho^+ l^- \bar{\nu}_l$ and from the second they obtain results for $\bar{B} \rightarrow K^* \gamma$. The combined fit in the K^* case is illustrated in Figure 12. The figure demonstrates the large extrapolation needed to reach $q^2 = 0$.

Our preferred results for $\bar{B}^0 \rightarrow \pi^+ l^- \bar{\nu}_l$ and $\bar{B}^0 \rightarrow \rho^+ l^- \bar{\nu}_l$ come from the UKQCD constrained fits⁹¹. Their values for the form factors extrapolated to $q^2 = 0$ agree well with light-cone sum rule calculations, which work best at low q^2 . The fitted form factors also agree with experimental results for the rates and ratio-of-rates of these semileptonic decays. However, we emphasise that the extrapolated form factors are no longer model independent.

There are also preliminary results for heavy-to-light form factors from FNAL, JLQCD and a Hiroshima-KEK group (see the reviews in^{10,11}) and the different lattice calculations are in agreement for the form factors at large q^2 where they are measured.

Table 13 lists the values of $T(0) \equiv T_1(0) = iT_2(0)$ for $\bar{B} \rightarrow K^* \gamma$, together with the directly measured $T_2(q_{\text{max}}^2)$. All groups find that T_2 has much less

^fIn the extrapolation of the raw lattice results to the B -meson mass, this analysis also applies the condition in Eq. (55), that the pairs $(V, 2T_1)$ and $(A_1, 2iT_2)$ should agree at fixed ω in the infinite heavy mass limit.

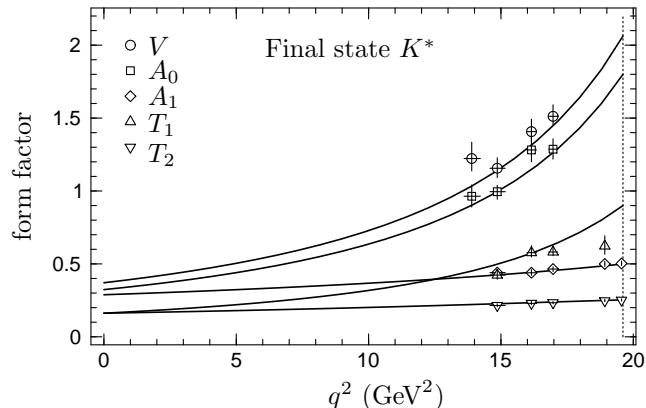


Figure 12: UKQCD⁹¹ fit to the lattice predictions for A_0 , A_1 , V , T_1 and T_2 for a K^* meson final state assuming a pole form for A_1 . A_2 is not reliably extracted from the lattice data so is not used in the fit. The dashed vertical line indicates q_{\max}^2 .

q^2 dependence than T_1 , although the lattice data again do not themselves distinguish a preferred q^2 dependence. In order to make a distinction, one can apply the light-cone sum rule scaling relation at $q^2 = 0$, see Eq. (61), which states that $T(0)$ has a leading $M^{-3/2}$ behaviour. In the table we list results from form factor fits which satisfy this scaling law. Our preference is to quote the UKQCD⁹¹ result (with statistical error only) from the combined fit to $B \rightarrow V$ decays described above:

$$T(0) = 0.16 \binom{2}{1}. \quad (62)$$

Using this value to evaluate the ratio (given at leading order in QCD and up to $O(1/m_b^2)$ corrections¹⁰³)

$$R_{K^*} = \frac{\Gamma(\bar{B} \rightarrow K^* \gamma)}{\Gamma(b \rightarrow s \gamma)} = 4 \left(\frac{m_B}{m_b} \right)^3 \left(1 - \frac{m_{K^*}^2}{m_B^2} \right)^3 |T(0)|^2 \quad (63)$$

results in

$$R_{K^*} = 16 \binom{4}{3} \%, \quad (64)$$

which is consistent with the experimental result 18(7)% from CLEO⁹³. Discrepancies between R_{K^*} calculated using $T(0)$ and the experimental ratio $\Gamma(\bar{B} \rightarrow K^* \gamma)/\Gamma(b \rightarrow s \gamma)$ could reveal the existence of long-distance effects in the exclusive decay. It has been proposed that these effects may be significant for the process $\bar{B} \rightarrow K^* \gamma$ ^{104–106}, but within the precision of the experimental and lattice results, there is no evidence for them.

Table 13: Lattice results for $\bar{B} \rightarrow K^* \gamma$. Values for $T(0) \equiv T_1(0) = iT_2(0)$ are quoted only from models which satisfy the light-cone sum rule scaling relation, Eq. (61), at $q^2 = 0$.

| | Yr | β | c_{sw} | norm | $T(0)$ | $T_2(q_{\text{max}}^2)$ |
|---------------------|----|---------|-----------------|------|-----------------------------------|-------------------------|
| UKQCD ⁹¹ | 97 | 6.2 | 1 | rel | 0.16(₁ ²) | 0.25(2) |
| LANL ¹⁰⁷ | 96 | 6.0 | 0 | nr | 0.09(1) | |
| APE ¹⁰⁸ | 96 | 6.0 | 1 | rel | 0.09(1)(1) | |
| BHS ¹⁰⁹ | 94 | 6.0 | 0 | nr | 0.101(10)(28) | 0.325(33)(65) |

5 The Parameters of the HQET

The Heavy Quark Effective Theory (HQET) is proving to be a particularly useful tool for phenomenological studies in charm and beauty physics, for reviews and references to the original literature see ^{72,110,111}. In this approach, physical quantities are calculated as series in inverse powers of the mass(es) of the heavy quark(s). The non-perturbative strong interaction effects can be parametrized in terms of matrix elements of local operators, which appear as factors in the expansion coefficients. Lattice simulations of the HQET provide the opportunity of computing these matrix elements numerically and in this section we briefly describe some of these calculations. We start with a general discussion (for a more detailed presentation and references to the original literature see Ref. ¹¹²) and then we will illustrate the main points by some important examples.

Consider some physical quantity \mathcal{P} which, using the operator product expansion can be written as a series in inverse powers of the mass of the heavy quark, m_Q ,⁹

$$\mathcal{P} = C_1(m_Q^2/\mu^2) \langle f | O_1(\mu) | i \rangle + \frac{C_2(m_Q^2/\mu^2)}{m_Q^n} \langle f | O_2(\mu) | i \rangle + O(1/m_Q^{n+p}), \quad (65)$$

where $n \geq 1$ and the coefficient functions C_i are independent of the states $|i\rangle$ and $|f\rangle$. The operators $O_{1,2}$ are composite operators of static heavy quark, light quark and gluon fields, renormalized at a scale μ . For clarity of notation, we suppress the dependence of the coefficient functions on the coupling constant, $\alpha_s(m_Q^2)$. We assume here that there is only one operator in each of the first two orders of the expansion. If this is not the case, then there is an additional mixing of operators, which requires only a minor modification of the discussion below. We will therefore not consider this possibility further. The

⁹For simplicity we assume that \mathcal{P} depends only on the mass of one heavy quark.

final term of $O(1/m_Q^{n+p})$ in Eq. (65) represents the contributions of operators of even higher dimension which will not be discussed here.

Throughout this discussion we assume that we wish to evaluate the contributions of $O((\Lambda_{\text{QCD}}/m_Q)^n)$ to \mathcal{P} , or at least to improve the precision given by the lowest order contribution.

In lattice simulations we work directly with bare operators (corresponding to the lattice regularization), so that the renormalization scale μ in Eq. (65) should be replaced by the cut-off a^{-1} . With a hard ultra-violet cut-off, such as the lattice spacing, the higher dimensional operators $O_{2,3,\dots}$ can mix with lower dimensional ones, and with O_1 in particular. By dimensional arguments it can readily be seen that the mixing coefficients will diverge as inverse powers of the lattice spacing. This implies, for example, that

$$\langle f | O_2(a) | i \rangle = O(a^{-n}) , \quad (66)$$

and so this matrix element, computed in lattice simulations, is clearly not a physical quantity. These power divergences are subtracted in the perturbative matching procedure in which the Wilson coefficient functions are computed; specifically the coefficient function C_1 contains terms of $O((ma)^{-n})$, which cancel the power divergences present in $\langle f | O_2 | i \rangle$. The perturbative series for C_1 is evaluated only at some low order (typically one loop). Since $(1/m_Q a)^n$ is much larger than $(\Lambda_{\text{QCD}}/m_Q)^n$, which is the order of the terms we are trying to evaluate, the truncation of the perturbative series for C_1 leads to a significant loss of precision^{*h*}. This is the principal problem, in attempts to quantify power corrections to hard scattering and decay amplitudes in general. We mention in passing that although the discussion here is in the context of lattice calculations, analogous problems occur also in the continuum regularization schemes, such as dimensional regularization¹¹².

In some cases the operator O_2 is protected from mixing under renormalization with O_1 , because of the presence of some symmetry. An important example of this in heavy quark physics is the chromomagnetic operator $\bar{h}\sigma_{ij}G^{ij}h$ (where h is the field of a static quark and $G^{\mu\nu}$ is the gluon field strength tensor), which cannot mix with the lower dimensional operator $\bar{h}h$ because it has a different spin structure. In such cases the corresponding problem of power divergences (and renormalon singularities) does not arise. For the remainder of the discussion we assume that O_2 and O_1 have the same quantum numbers, so that they can mix under renormalization. Another important exception to the general discussion is the difference of matrix elements of the kinetic energy operator taken between different hadronic states. In this case the higher dimensional operator, $\bar{h}\mathbf{D}^2h$, can mix with the lower dimensional one, $\bar{h}h$, but

^{*h*}The connection of the power divergences and renormalons is explained in Refs.^{112–114}.

as the latter is a conserved current it has the same matrix element between all single hadron states. Thus the corresponding power divergences cancel in the difference of matrix elements. In all of these exceptions the matrix elements of the higher dimensional operators (or linear combinations of matrix elements) are also the leading contribution to some physical quantity (for example, the chromomagnetic operator gives the leading contribution to the B^*-B mass splitting).

In the following subsections we consider 3 parameters which occur frequently in the evaluation of physical quantities using the HQET:

- $\bar{\Lambda}$, the binding energy of a heavy quark in a heavy hadron;
- λ_1 , the kinetic energy of the heavy quark;
- λ_2 , the matrix element of the chromomagnetic operator.

The binding energy $\bar{\Lambda}$ is defined as the difference of the masses of the heavy hadron and the heavy quark. In practice, the heavy quark mass must be defined at short distances (otherwise experimentally measurable quantities cannot be expressed in terms of the mass using perturbation theory), and below we will use the $\overline{\text{MS}}$ mass. The usefulness of introducing $\bar{\Lambda}$ is then unclear, and we present the discussion simply in terms of the mass itself. In all the three examples to be discussed below, results are presented from lattice calculations using static heavy quarks.

5.1 The Evaluation of the Mass of a Heavy Quark

The first example which we consider is the determination of the mass of a heavy quark (e.g. the b -quark), up to, and including the terms of $O(\Lambda_{\text{QCD}})$, but neglecting terms of $O(\Lambda_{\text{QCD}}^2/m_b)^i$.

In section 2, the computation of the decay constant of a meson containing a static heavy quark was discussed. This parameter is obtained by evaluating correlation functions of the form:

$$C(t) = \sum_{\mathbf{x}} \langle 0 | A_4(\mathbf{x}, t) A_4(\mathbf{0}, 0) | 0 \rangle \quad (67)$$

in lattice simulations of the HQET, with Lagrangian density

$$\mathcal{L} = \bar{h} D_4 h \ , \quad (68)$$

ⁱA formulation of this problem in terms of an explicit operator product expansion can be found in Refs. ^{115,113}.

where h represents the field of the static quark. For sufficiently large values of the time t ,

$$C(t) \simeq Z^2 e^{-\mathcal{E}t} + \dots, \quad (69)$$

where the ellipsis represents contributions from excited states. The value of f_B in the static limit is obtained from the prefactor Z . In addition, however, from the exponent \mathcal{E} it is possible to obtain the $O(\Lambda_{\text{QCD}})$ contribution to m_b . Performing the matching of the heavy quark propagator in full QCD and in the HQET gives¹¹⁶

$$\mathcal{E} = m_B - (m_b^{\text{pole}} - \delta m), \quad (70)$$

where m_B is the mass of the B -meson and m_b^{pole} is the pole mass of the b -quark. Although we have chosen the bare Lagrangian (68) to have no mass term, higher order perturbative corrections generate such a term and

$$\delta m = \sum_{n=1}^{\infty} \left(\frac{\alpha_s}{4\pi} \right)^n \frac{X_n}{a} \quad (71)$$

represents the perturbation series generating the mass. Both \mathcal{E} and δm diverge linearly with the lattice spacing, so that they are not physical quantities. m_b^{pole} is also unphysical, and in perturbation theory contains renormalon ambiguities^{115,117}. These ambiguities cancel those also present in δm in the difference on the right-hand side of Eq. (70). Thus it is possible to determine the value of a physical (short-distance) definition of the quark mass, such as $\overline{m}_b \equiv \overline{m}_b^{\overline{MS}}(m_b^{\overline{MS}})$ from the computed value of \mathcal{E} . In practice, however, the subtraction of the linear divergence, which is performed in perturbation theory leads to large numerical cancellations and hence to significant uncertainties. In reference¹¹⁸ it was found that

$$\overline{m}_b = 4.15 \pm 0.05 \pm 0.20 \text{ GeV}. \quad (72)$$

The first error on the right-hand side of Eq. (72) is due to uncertainties in the lattice evaluation of \mathcal{E} and in the value of the lattice spacing. However, the larger error of 200 MeV or so is the estimate of the uncertainty due to the truncation of the perturbation series for δm at one-loop order. Evaluation of higher order terms in this series, perhaps using the methods developed in Ref.¹¹⁹, based on the Langevin stochastic formulation of lattice QCD, is urgently needed to reduce the uncertainty in the computed value of \overline{m}_b .

5.2 Kinetic Energy of a Heavy Quark

The next example which we will consider is the evaluation of the kinetic energy of the heavy quark λ_1 , which appears in many applications of the HQET⁷².

On the lattice we start with the evaluation of the matrix element of the bare operator

$$\lambda_1^{\text{bare}} = - \frac{\langle B | \bar{h}(i\mathbf{D})^2 h | B \rangle}{2M_B} \quad (73)$$

$$= -(0.69 \pm 0.03 \pm 0.03) a^{-2} \quad (74)$$

where the numerical result is taken from a simulation on a $24^3 \times 60$ lattice at $\beta = 6.0$ with the SW-action¹²⁰. Taking the lattice spacing to be 2.0 ± 0.2 GeV, we see that the magnitude of the result is about 2.8 GeV^2 , to be compared to the expected physical corrections of $O(\Lambda_{\text{QCD}}^2) \sim 0.1 \text{ GeV}^2$. Of course, the large result is due to the presence of power divergences, in this case they are quadratic, i.e. they are of $O(a^{-2})$. In one-loop perturbation theory, the power divergence is equal to $-5.19 \alpha_s a^{-2}$, which, depending on the value taken for the coupling constant α_s , is in the range $(0.67 - 0.93)a^{-2}$ (the choice of a suitable definition of the coupling constant is a representation of our ignorance of the higher order perturbative corrections, the range given here comes from frequently used definitions). The uncertainty is greater than the terms we are trying to evaluate which are of $O(\Lambda_{\text{QCD}}^2)$. Clearly, in order for the lattice result to be useful for phenomenological applications, the perturbative calculations must be performed to higher orders, which is the main conclusion of this subsection.

It is also possible to subtract the power divergences non-perturbatively. In Refs.^{113,116,120} a subtracted kinetic energy operator,

$$\bar{h}\mathbf{D}_S^2 h \equiv \bar{h}\mathbf{D}^2 h - \frac{c}{a^2} \bar{h}h, \quad (75)$$

was defined, with the subtraction constant c fixed by imposing that the matrix element of this operator vanishes between quark states at rest (in the Landau Gauge). The corresponding value of λ_1 , which is now free of quadratic divergences, was found to be^j

$$\lambda_1 = a^{-2} Z_{\mathbf{D}_S^2} (a^2 \lambda_1^{\text{bare}} - a^2 c) \quad (76)$$

$$= 0.09 \pm 0.14 \text{ GeV}^2. \quad (77)$$

Of course the large relative error in Eq. (77) is due to the large cancellation between the two terms in the parentheses in Eq. (76). In Eq.(76), $Z_{\mathbf{D}_S^2}$ is the normalization constant required to obtain the continuum, $\overline{\text{MS}}$, value of λ_1 from the subtracted lattice one.

^jNote that the central value in Eq. (77) has the opposite sign to that of many other estimates using various definitions of λ_1 .

The difficulties described here arise because of the mixing of the kinetic energy operator $\bar{h}(i\mathbf{D})^2h$ with $\bar{h}h/a^2$. Since $\bar{h}h$ is a conserved current in the HQET, its matrix elements are the same between all hadronic states. This means that the difference of the matrix elements of the kinetic energy operator between any two different beauty hadrons is a physical quantity, and for example in Ref. ¹²⁰ it was found that

$$\lambda_1(B_s) - \lambda_1(B_d) = -0.09 \pm 0.04 \text{ GeV}^2 . \quad (78)$$

This difference is the leading contribution to the following combination of masses

$$\lambda_1(B_s) - \lambda_1(B_d) = \frac{\bar{m}_{B_s} - \bar{m}_{B_d} - (\bar{m}_{D_s} - \bar{m}_{D_d})}{\frac{1}{2} \left(\frac{1}{m_D} - \frac{1}{m_B} \right)} + O \left(\frac{\Lambda_{\text{QCD}}^3}{m_Q} \right) , \quad (79)$$

where, for example, \bar{m}_B is the spin averaged mass of the B -meson (with the corresponding light valence quark)

$$\bar{m}_B = \frac{1}{4} (3m_{B^*} + m_B) , \quad (80)$$

and m_Q is the mass of the heavy quark Q ($Q = b$ or c). Where appropriate, we have included the subscript d or s to denote the presence of the corresponding light valence quark. The experimental value of the first term on the right hand side of Eq. (79) is $-0.06 \pm 0.02 \text{ GeV}^2$, in very good agreement with the result in Eq. (78). It must however be remembered that the $O(\Lambda_{\text{QCD}}^3/m_c)$ corrections to this result may be significant.

5.3 λ_2 ; The Matrix Element of the Chromomagnetic Operator

The chromomagnetic operator $\bar{h}\frac{1}{2}\sigma_{ij}G^{ij}h$, does not mix with the operator $\bar{h}h$, and hence its matrix elements are free of power divergences. The parameter λ_2 , defined as

$$\lambda_2 \equiv \frac{1}{2m_B} \frac{1}{3} \langle B | \bar{h} \frac{1}{2} \sigma_{ij} G^{ij} h | B \rangle \quad (81)$$

gives the first term in the hyperfine splitting in the B -meson system:

$$m_{B^*}^2 - m_B^2 = 4\lambda_2 . \quad (82)$$

The lattice results for λ_2 are all significantly smaller (by almost a factor of two) than the values deduced from the physical masses of the B^* and B mesons. In two recent lattice computations the authors found:

$$m_{B^*}^2 - m_B^2 = \begin{cases} 0.28 \pm 0.02 \pm 0.04 \text{ GeV}^2 & \text{Ref. }^{54} \\ 0.28 \pm 0.06 \text{ GeV}^2 & \text{Ref. }^{120} \end{cases} \quad (83)$$

to be compared to the experimental value of $0.485 \pm 0.005 \text{ GeV}^2$, see Ref. ¹²¹.

One possible source for the discrepancy between the lattice results and the experimental value is the unusually large one-loop contribution to the renormalization constant relating the lattice and continuum chromomagnetic operator ¹²². This renormalization constant is about 1.85 at one-loop order, and so one may wonder whether the higher order terms might give a significant contribution. Other possible contributions to the discrepancy might be the use of the quenched approximation, or that the relation between λ_2 and the hyperfine splitting may be significantly modified by higher order corrections in $1/m_b$. It is important to clarify the source of this discrepancy.

Lattice calculations of the hyperfine splitting using propagating heavy quarks also give a result which is smaller than the experimental one. This is a different problem, however, which is related to the presence of a spurious chromomagnetic term of $O(a)$ present in the lattice action. This interpretation is confirmed by the fact that the computed value of the splitting increases as the action is “improved” in agreement with expectations ^{123,124}.

6 Exclusive Non-Leptonic Decays of Heavy Mesons

Exclusive non-leptonic decays are, in principle, an important source of fundamental information on the properties of weak decays of heavy quarks. Unfortunately our current theoretical understanding of the non-perturbative QCD effects in these processes is rather primitive, and we are forced to make assumptions based on factorization and/or quark models ¹²⁵. Lattice computations of the corresponding matrix elements are also difficult ¹²⁶. They need to be performed in Euclidean space, where there is no distinction between *in*- and *out*-states. The quantities which one obtains directly in lattice computations are the (real) averages such as

$$\langle M_1 M_2 | \mathcal{H}_W | B \rangle = \frac{1}{2} \left({}_{\text{in}} \langle M_1 M_2 | \mathcal{H}_W | B \rangle + {}_{\text{out}} \langle M_1 M_2 | \mathcal{H}_W | B \rangle \right), \quad (84)$$

where M_1 and M_2 are mesons. It is therefore not possible to obtain directly any information about the phase due to final state interactions, and hence to determine the matrix elements reliably. Maiani and Testa ¹²⁶ also showed that the quantities which are obtained from the large time behaviour of the corresponding correlation functions are the unphysical form factors in which the final state mesons are at rest, e.g.

$$\langle M_1(\mathbf{p}_{M_1} = \mathbf{0}) M_2(\mathbf{p}_{M_2} = \mathbf{0}) | \mathcal{H}_W | B \rangle. \quad (85)$$

For $K \rightarrow \pi\pi$ decays chiral perturbation theory can then be used to obtain the physical form factors with reasonable accuracy. For D - and B -meson decays this is not possible.

The publication of the Maiani-Testa¹²⁶ theorem stopped the exploratory work on the numerical evaluation of two-body non-leptonic decays. These early, and not very accurate papers, studied the non-penguin contributions to D -meson decay amplitudes¹²⁷.

The Maiani-Testa theorem implies that it is not possible to obtain the phase of the final state interactions without some assumptions about the amplitudes. The importance of developing reliable quantitative techniques for the evaluation of non-perturbative QCD effects in non-leptonic decays cannot be overstated, and so attempts to introduce “reasonable” assumptions to enable calculations to be performed (and compared with experimental data) are needed urgently. Ciuchini et al.^{128,129} have recently shown that by making a “smoothness” hypothesis about the decay amplitudes it is possible to extract information about the phase of two-body non-leptonic amplitudes. Studies to see whether their proposals are practicable and consistent are currently beginning.

7 Conclusions

The decays of heavy quarks, and the b -quark in particular, provide a powerful laboratory to test the standard model of particle physics, to determine its parameters (in particular, the elements of the CKM-matrix) and to look for signatures of new physics. Non-perturbative QCD effects in these weak decays are the major difficulty in interpreting the present and future experimental data. Lattice computations provide the opportunity to quantify these effects, and much effort is being devoted to the evaluation of the decay amplitudes of heavy quarks. In this article we have reviewed the status of these calculations, presenting an overview of the results for leptonic decay constants, the amplitudes for $B - \bar{B}$ mixing, the form factors for semileptonic and rare radiative decays and the parameters $\bar{\Lambda}$, λ_1 and λ_2 of the HQET. These successful calculations are playing a central rôle in phenomenological studies.

As explained in Section 6, relatively little progress has been achieved so far in understanding exclusive non-leptonic decays on the lattice, or indeed any physical process in which there are two hadrons in the initial or final state. It is very important to try to overcome the theoretical difficulties which have so far prevented this very important class of processes from being amenable to study in lattice simulations.

Lattice simulations are a “first principles” non-perturbative technique for

the evaluation of the strong interaction effects in weak decay amplitudes (and in those of heavy quarks in particular). However, the precision of the results is limited by the available computing resources, and the priority is to reduce and control the systematic uncertainties, especially those due to the quenched approximation. This is discussed in some detail in Section 1.2 above. During the next few years, studies with dynamical fermions will continue and improve, enabling us to begin seriously quantifying the effects of the quenched approximation. The very significant progress achieved in recent years in reducing the errors due to the finiteness of the lattice spacing, makes this task easier, allowing for meaningful studies on coarser lattices than would otherwise be the case. Once precise studies with dynamical quarks become possible, lattice QCD together with large scale numerical simulations will be a truly and fully quantitative technique for the evaluation of the effects of the strong interactions, with no model assumptions or parameters. Although this will still take a few years, we have tried to demonstrate in this review that lattice simulations, with their expected $O(10\text{--}20\%)$ systematic uncertainties for most physical quantities, are already a most reliable and useful tool.

Acknowledgements

We warmly thank B. Hill, L.P. Lellouch, G. Martinelli, J. Nieves, H. Wittig and all our colleagues from the APE, ELC, FNAL and UKQCD collaborations from whom we have learned so much. We also thank C. Bernard, V. Braun, P. Drell, S. Gottlieb, S. Güsken, S. Hashimoto, H. Hoerber, P. Mackenzie, T. Onogi, A. Ryd and R. Zaliznyak for their help in clarifying important questions.

We acknowledge support from the Particle Physics and Astronomy Research Council, UK, through grants GR/K55738 and GR/L22744.

References

1. C.T. Sachrajda, Proc. Lattice 92, 10th Int. Symp. on Lattice Field Theory, Amsterdam, Netherlands, 1992, Nucl. Phys. B (Proc. Suppl.) **30** (1993) 20
2. P.B. Mackenzie, Proc. Lattice 92, 10th Int. Symp. on Lattice Field Theory, Amsterdam, Netherlands, 1992, Nucl. Phys. B (Proc. Suppl.) **30** (1993) 35
3. C.W. Bernard, Proc. Lattice 93, 11th Int. Symp. on Lattice Field Theory, Dallas, Texas, 1993, Nucl. Phys. B (Proc. Suppl.) **34** (1994) 47
4. R.D. Kenway, Proc. Lattice 93, 11th Int. Symp. on Lattice Field Theory, Dallas, Texas, 1993, Nucl. Phys. B (Proc. Suppl.) **34** (1994) 153

5. G. Martinelli, Proc. Lattice 94, 12th Int. Symp. on Lattice Field Theory, Bielefeld, Germany, 1994, Nucl. Phys. B (Proc. Suppl.) **42** (1995) 127
6. R. Sommer, Proc. Lattice 94, 12th Int. Symp. on Lattice Field Theory, Bielefeld, Germany, 1994, Nucl. Phys. B (Proc. Suppl.) **42** (1995) 186
7. J.N. Simone, Proc. Lattice 95, 13th Int. Symp. on Lattice Field Theory, Melbourne, Australia, 1995, Nucl. Phys. B (Proc. Suppl.) **47** (1996) 17
8. C.R. Allton, Proc. Lattice 95, 13th Int. Symp. on Lattice Field Theory, Melbourne, Australia, 1995, Nucl. Phys. B (Proc. Suppl.) **47** (1996) 31
9. A. Soni, Proc. Lattice 95, 13th Int. Symp. on Lattice Field Theory, Melbourne, Australia, 1995, Nucl. Phys. B (Proc. Suppl.) **47** (1996) 43
10. J.M. Flynn, Proc. Lattice 96, 14th Int. Symp. on Lattice Field Theory, St Louis, USA, 1996, Nucl. Phys. B (Proc. Suppl.) **53** (1997) 168
11. T. Onogi, to appear in Proc. Lattice 97, 15th Int. Symp. on Lattice Field Theory, Edinburgh, Scotland, 1997
12. C.T.H. Davies, Glasgow preprint GUTPA-97-05-2, hep-lat/9705039
13. B.A. Thacker and G.P. Lepage, Phys. Rev. D **43** (1991) 196
14. K. Symanzik, in Mathematical Problems in Theoretical Physics, eds. R. Schrader et al., Lecture Notes in Physics vol. 153 (Springer, New York, 1982); Nucl. Phys. B **226** (1983) 187; Nucl. Phys. B **226** (1983) 205
15. M. Lüscher and P. Weisz, Commun. Math. Phys. **97** (1985) 59; erratum Commun. Math. Phys. **98** (1985) 433
16. B. Sheikholeslami and R. Wohlert, Nucl. Phys. B **259** (1985) 572
17. G. Heatlie et al., Nucl. Phys. B **352** (1991) 266
18. M. Lüscher et al., Nucl. Phys. B **478** (1996) 365; M. Lüscher and P. Weisz, Nucl. Phys. B **479** (1996) 429; M. Lüscher et al., Nucl. Phys. B **491** (1997) 323
19. G. Martinelli et al., Edinburgh-Rome 1-Rome 2-Southampton-Seattle preprint, Edinburgh 96/28, Rome-1 1159/97, ROM2F-20/97, SHEP 97-05, UW/PT 96-33, hep-lat/9705018
20. K.G. Wilson, Phys. Rev. D **10** (1974) 2445; K.G. Wilson, in New Phenomena in Subnuclear Physics, ed. A. Zichichi (Plenum Press, New York, 1975) p. 69
21. P. Lacey et al., Phys. Rev. D **51** (1995) 6403
22. M. Bochicchio et al., Nucl. Phys. B **262** (1985) 331; L.H. Karsten and J. Smit, Nucl. Phys. B **183** (1981) 103; L. Maiani and G. Martinelli, Phys. Lett. B **178** (1986) 265; G. Martinelli, S. Petrarca, C. T. Sachrajda and A. Vladikas, Phys. Lett. B **311** (1993) 241; erratum Phys. Lett. B **317** (1993) 660
23. G. Martinelli, C. Pittori, C.T. Sachrajda, M. Testa and A. Vladikas, Nucl. Phys. B **445** (1995) 81

24. M. Lüscher, S. Sint, R. Sommer and H. Wittig, Nucl. Phys. B **491** (1997) 344
25. SESAM and T χ L Collaborations, H. Hoerber et al., Proc. Lattice 97, 15th Int. Symp. on Lattice Field Theory, Edinburgh, Scotland, 1997, hep-lat/9709137
26. MILC Collaboration, C. Bernard et al., Proc. Lattice 97, 15th Int. Symp. on Lattice Field Theory, Edinburgh, Scotland, 1997, hep-lat/9709142
27. JLQCD Collaboration, S. Aoki et al., talk presented at Lattice 97, 15th Int. Symp. on Lattice Field Theory, Edinburgh, Scotland, 1997
28. APE Collaboration, C.R. Allton et al., Rome–SNS–Swansea preprint, ROME–97/1164, SNS/PH/1997–005, SWAT/148, hep-lat/9703002
29. T. Bhattacharya and R. Gupta, Phys. Rev. D **54** (1996) 1155
30. C. Alexandrou et al., Z. Phys C **62** (1994) 659
31. UKQCD Collaboration, R.M. Baxter et al., Phys. Rev. D **49** (1994) 1594
32. C.W. Bernard, J.N. Labrenz and A. Soni, Phys. Rev. D **49** (1994) 2536
33. HEMCGC Collaboration, K.M. Bitar et al., Phys. Rev. D **49** (1994) 3546
34. HEMCGC Collaboration, K.M. Bitar et al., Phys. Rev. D **48** (1993) 370
35. ELC Collaboration, A. Abada et al., Nucl. Phys. B **376** (1992) 172
36. C. Alexandrou et al., Phys. Lett. B **256** (1991) 60
37. ELC Collaboration, M.B. Gavela et al., Phys. Lett. B **206** (1988) 113
38. T.A. DeGrand and R.D. Loft, Phys. Rev. D **38** (1988) 954. Note that the decay constants quoted in this paper have been multiplied by $\sqrt{2}$ to convert to the normalization used here.
39. C. Bernard et al., Phys. Rev. D **38** (1988) 3540
40. A. Kronfeld, Proc. Lattice 92, 10th Int. Symp. on Lattice Field Theory, Amsterdam, Netherlands, 1992, Nucl. Phys. B (Proc. Suppl.) **30** (1993) 445
41. G.P. Lepage and P.B. Mackenzie, Nucl. Phys. B (Proc. Suppl.) **20** (1992) 173
42. G.P. Lepage and P.B. Mackenzie, Phys. Rev. D **48** (1993) 2250
43. A.X. El-Khadra, A.S. Kronfeld and P.B. Mackenzie, Phys. Rev. D **55** (1997) 3933
44. H. Wittig, Oxford preprint OUTFP–97–20P, to appear in Int. J. Mod. Phys., hep-lat/9705034
45. S.R. Sharpe and Y. Zhang, Phys. Rev. D **53** (1996) 5125
46. S.R. Sharpe, Proc. Lattice 96, 14th Int. Symp. on Lattice Field Theory, St Louis, USA, 1996, Nucl. Phys. B (Proc. Suppl.) **53** (1997) 181
47. APETOV Collaboration, G.M. de Divitiis et al., Phys. Lett. B **382** (1996) 398
48. R. Sommer, Phys. Rep. **275** (1996) 1

49. J. Richman, Proc. ICHEP96, 28th Int. Conf. on High Energy Physics, Warsaw, Poland, 25–31 July 1996, edited by Z. Ajduk and A.K. Wroblewski, World Scientific, Singapore (1997) p. 143
50. A. J. Buras and R. Fleischer, this volume, hep-ph/9704376
51. A.J. Buras, M. Jamin and P.H. Weisz, Nucl. Phys. B **347** (1990) 491
52. V. Giménez and G. Martinelli, Phys. Lett. B **398** (1997) 135
53. J. Christensen, T. Draper and C. McNeile, Kentucky preprint UK-96-11, hep-lat/9610026
54. UKQCD Collaboration, A.K. Ewing et al., Phys. Rev. D **54** (1996) 3526
55. J.M. Flynn, O.F. Hernández and B.R. Hill, Phys. Rev. D **43** (1991) 3709
56. A. Borrelli and C. Pittori, Nucl. Phys. B **385** (1992) 502; A. Borrelli, C. Pittori, R. Frezzotti and E. Gabrielli, Nucl. Phys. B **409** (1993) 382
57. V. Giménez, Nucl. Phys. B **401** (1993) 116
58. M. Ciuchini, E. Franco and V. Giménez, Phys. Lett. B **388** (1996) 167
59. G. Buchalla, Phys. Lett. B **395** (1997) 364
60. C. Bernard, T. Blum and A. Soni, Proc. Lattice 96, 14th Int. Symp. on Lattice Field Theory, St Louis, USA, 1996, Nucl. Phys. B (Proc. Suppl.) **53** (1997) 382
61. JLQCD Collaboration, S. Aoki et al., Proc. Lattice 95, 13th Int. Symp. on Lattice Field Theory, Melbourne, Australia, 1995, Nucl. Phys. B (Proc. Suppl.) **47** (1996) 433
62. C. Bernard, hep-ph/9709460, to be published in Proc. Seventh Int. Symp. on Heavy Flavour Physics, Santa Barbara, July 1997
63. UKQCD Collaboration, K.C. Bowler et al., Phys. Rev. D **51** (1995) 4905
64. S. Güsken, private communication, paper in preparation
65. T. Bhattacharya and R. Gupta, Proc. Lattice 94, 12th Int. Symp. on Lattice Field Theory, Bielefeld, Germany, 1994, Nucl. Phys. B (Proc. Suppl.) **42** (1995) 935
66. T. Bhattacharya and R. Gupta, Proc. Lattice 95, 13th Int. Symp. on Lattice Field Theory, Melbourne, Australia, 1995, Nucl. Phys. B (Proc. Suppl.) **47** (1996) 481
67. APE Collaboration, C.R. Allton et al., Phys. Lett. B **345** (1995) 513
68. A. Ryd, talk presented at Seventh Int. Symp. on Heavy Flavours, Santa Barbara, California, July 1997
69. As. Abada et al., Nucl. Phys. B **416** (1994) 675
70. C. Bernard, A.X. El-Khadra and A. Soni, Phys. Rev. D **43** (1991) 2140; Phys. Rev. D **45** (1992) 869

71. M. Crisafulli, G. Martinelli, V.J. Hill and C.T. Sachrajda, Phys. Lett. B **223** (1989) 90; V. Lubicz, G. Martinelli and C.T. Sachrajda, Nucl. Phys. B **356** (1991) 301; V. Lubicz, G. Martinelli, M.S. McCarthy and C.T. Sachrajda, Phys. Lett. B **274** (1992) 415
72. M. Neubert, this volume, hep-ph/9702375
73. L.K. Gibbons, Proc. ICHEP96, 28th Int. Conf. on High Energy Physics, Warsaw, Poland, 25–31 July 1996, edited by Z. Ajduk and A.K. Wroblewski, World Scientific, Singapore (1997) p. 183
74. M. Luke, Phys. Lett. B **252** (1990) 447
75. UKQCD Collaboration, K.C. Bowler et al., Phys. Rev. D **52** (1995) 5067
76. L. Lellouch, presented at 34th Cracow Sch. of Theor. Phys., Zakopane, Poland, 1994, Acta Phys. Polon. **B25** (1994) 1679
77. C.W. Bernard, Y. Shen and A. Soni, Proc. Lattice 93, 11th Int. Symp. on Lattice Field Theory, Dallas, Texas, 1993, Nucl. Phys. B (Proc. Suppl.) **34** (1994) 483; Phys. Lett. B **317** (1993) 164
78. CLEO Collaboration, B. Barish et al., Phys. Rev. D **51** (1995) 1014
79. M. Artuso, Nucl. Instrum. Meth. A **384** (1996) 39
80. J.E. Mandula and M.C. Ogilvie, Proc. Lattice 93, 11th Int. Symp. on Lattice Field Theory, Dallas, Texas, 1993, Nucl. Phys. B (Proc. Suppl.) **34** (1994) 480; preprint hep-lat/9408006
81. T. Draper and C. McNeile, Proc. Lattice 95, 13th Int. Symp. on Lattice Field Theory, Melbourne, Australia, 1995, Nucl. Phys. B (Proc. Suppl.) **47** (1996) 429; J. Christensen, T. Draper and C. McNeile, to appear in Proc. Lattice 97, 15th Int. Symp. on Lattice Field Theory, Edinburgh, Scotland, 1997, hep-lat/9710025
82. S. Hashimoto and H. Matsufuru, Phys. Rev. D **54** (1996) 4578
83. MILC Collaboration, C. Bernard et al., Proc. Lattice 97, 15th Int. Symp. on Lattice Field Theory, Edinburgh, Scotland, 1997, hep-lat/9709134
84. J.E. Mandula and M.C. Ogilvie, Phys. Rev. D **45** (1992) 2183
85. J.E. Mandula, Nucl. Phys. B (Proc. Suppl.) **30** (1993) 35
86. U. Aglietti, M. Crisafulli and M. Masetti, Phys. Lett. B **294** (1992) 281
87. UKQCD Collaboration, K.C. Bowler et al., Edinburgh–Granada–Marseille–Southampton preprint, Edinburgh 96/31, CPT–97/P.3459, UG–DFM–1/97, SHEP 97/14, hep-lat/9709028
88. J.R. Patterson, Proc. ICHEP96, 28th Int. Conf. on High Energy Physics, Warsaw, Poland, 25–31 July 1996, edited by Z. Ajduk and A.K. Wroblewski, World Scientific, Singapore (1997) p. 871
89. UKQCD Collaboration, D.R. Burford et al., Nucl. Phys. B **447** (1995) 425
90. UKQCD Collaboration, J.M. Flynn et al., Nucl. Phys. B **461** (1996) 327

91. UKQCD Collaboration, L. Del Debbio et al., Granada–Marseille–Southampton preprint, UG–DFM–4/97, CPT–97/P.3505, SHEP–97–13, hep-lat/9708008
92. CLEO Collaboration, R. Ammar et al., Phys. Rev. Lett. **71** (1993) 674
93. CLEO Collaboration, R. Ammar et al., preprint CLEO CONF 96–05 (1996)
94. N. Isgur and M. B. Wise, Phys. Rev. D **42** (1990) 2388
95. P.A. Griffin, M. Masip and M. McGuigan, Phys. Rev. D **42** (1994) 5751
96. L. Lellouch, Nucl. Phys. B **479** (1996) 353
97. D. Becirevic, LPTHE–Orsay preprint 97/16, hep-ph/9707271
98. V.M. Belyaev et al., Phys. Rev. D **51** (1995) 6177
99. P. Ball, Phys. Rev. D **48** (1993) 3190
100. A. Ali, V. Braun and H. Simma, Z. Phys C **63** (1994) 437.
101. P. Ball, Proc. 31st Rencontres de Moriond: Electroweak Interactions and Unified Theories, Les Arcs, France, March 1996, p. 365; V.M. Braun, Proc. Int. Europhysics Conf. on High Energy Physics, Brussels, Belgium, July 1995, p. 436; P. Ball and V.M. Braun, Phys. Rev. D **55** (1997) 5561
102. B. Stech, Phys. Lett. B **354** (1995) 447
103. M. Ciuchini et al., Phys. Lett. B **334** (1994) 137
104. E. Golowich and S. Pakvasa, Phys. Lett. B **205** (1988) 393
105. E. Golowich and S. Pakvasa, Phys. Rev. D **51** (1995) 1215
106. D. Atwood, B. Blok and A. Soni, Int. J. Mod. Phys. A **11** (1996) 3743
107. R. Gupta and T. Bhattacharya, Proc. Lattice 95, 13th Int. Symp. on Lattice Field Theory, Melbourne, Australia, 1995, Nucl. Phys. B (Proc. Suppl.) **47** (1996) 473
108. APE Collaboration, As. Abada et al., Phys. Lett. B **365** (1996) 275
109. C. Bernard, P. Hsieh and A. Soni, Phys. Rev. Lett. **72** (1994) 1402
110. M. Neubert, Phys. Rep. **245** (1994) 259
111. N. Isgur and M.B. Wise, in “Heavy Flavours”, (eds. A.J. Buras and M. Lindner, World Scientific, Singapore, 1992) 234
112. G. Martinelli and C.T. Sachrajda, Nucl. Phys. B **478** (1996) 660
113. G. Martinelli and C.T. Sachrajda, Phys. Lett. B **354** (1995) 423
114. C.T. Sachrajda, Proc. Lattice 95, 13th Int. Symp. on Lattice Field Theory, Melbourne, Australia, 1995, Nucl. Phys. B (Proc. Suppl.) **47** (1996) 100
115. M. Beneke and V.M. Braun, Nucl. Phys. B **426** (1994) 301
116. M. Crisafulli, V. Giménez, G. Martinelli and C.T. Sachrajda, Nucl. Phys. B **457** (1995) 594
117. I.I. Bigi, M.A. Shifman, N.G. Uraltsev and A.I. Vainshtein, Phys. Rev. D **50** (1994) 2234

118. V. Giménez, G. Martinelli and C.T. Sachrajda, Phys. Lett. B **393** (1997) 124
119. F. Di Renzo, E. Onofri and G. Marchesini, Nucl. Phys. B **457** (1995) 202
120. V. Giménez, G. Martinelli and C.T. Sachrajda, Nucl. Phys. B **486** (1997) 227
121. R.M. Barnett et al., Phys. Rev. D **54** (1996) 1
122. J.M. Flynn and B.R. Hill, Phys. Lett. B **264** (1991) 173
123. UKQCD Collaboration, C.R. Allton et al., Phys. Lett. B **292** (1992) 408
124. A.S. Kronfeld and P.B. Mackenzie, Ann. Rev. Nucl. Part. Sci. **43** (1993) 793
125. M. Neubert and B. Stech, this volume, hep-ph/9705292
126. L. Maiani and M. Testa, Phys. Lett. B **245** (1990) 585
127. C. Bernard, J. Simone and A. Soni, Nucl. Phys. B (Proc. Suppl.) **17** (1990) 504; As. Abada et al., Nucl. Phys. B (Proc. Suppl.) **17** (1990) 518
128. M. Ciuchini, E. Franco, G. Martinelli and L. Silvestrini, Phys. Lett. B **380** (1996) 353
129. L. Silvestrini, Nucl. Phys. A (Proc. Suppl.) **54** (1997) 276